may/june 1980 vol. 25, no. 3

PCI Journal

prestressed concrete institute

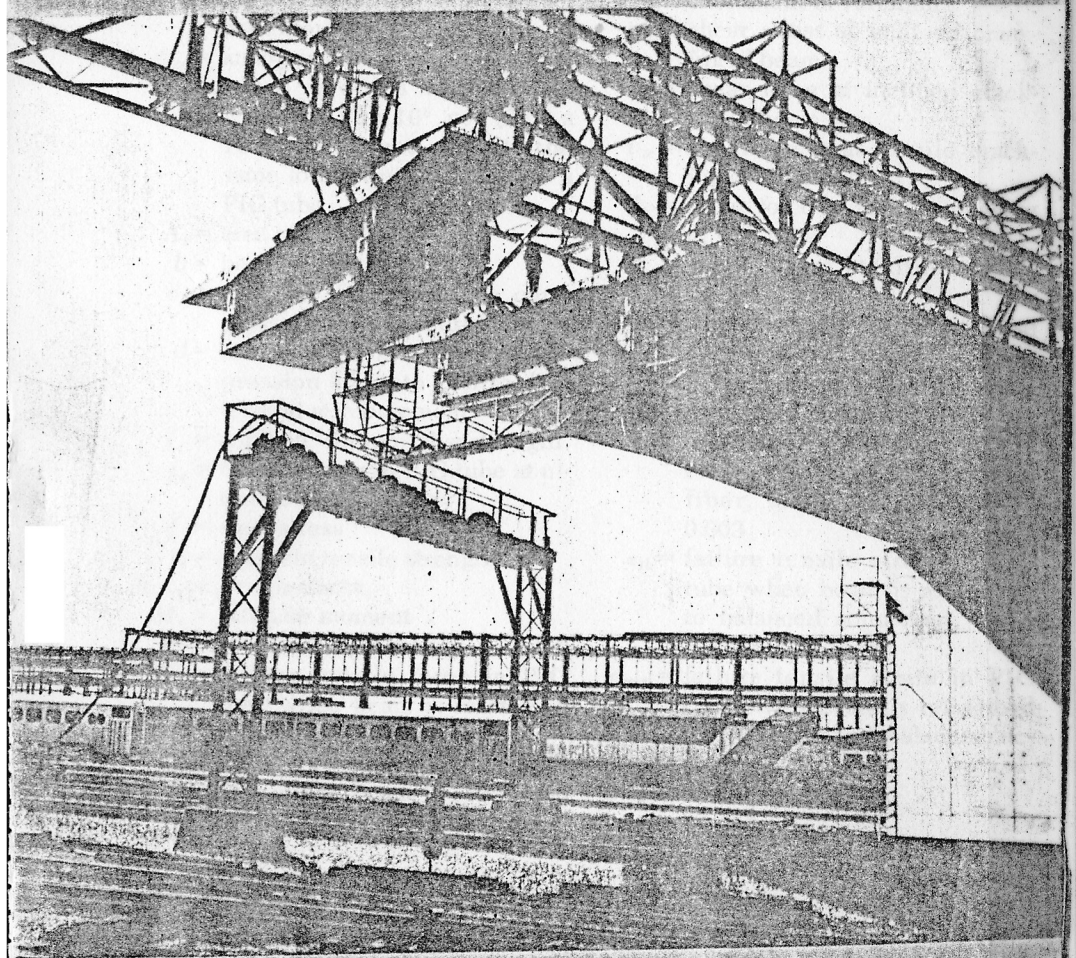

▶The Islington Avenue Bridge: Design/Construction, p. 32

Creep and Shrinkage Characterization for Analyzing Prestressed Concrete Structures

Zdeněk P. Bažant
Professor of Civil Engineering
Northwestern University
Evanston, Illinois

Liisa Panula*
Engineer, TAMS (Tippetts, Abbett, McCarthy and Stratton)
New York, N.Y.

Synopsis

Many prestressed concrete structures are sensitive to creep and shrinkage, necessitating accurate prediction. Creep and shrinkage characterization, and models for predicting its parameters, are analyzed, and a new simplified model is proposed.

Extensive graphical and statistical comparisons with test data available in the literature are made to verify and calibrate the model. The deviations of predictions made using existing ACI and CEB models from the same data are also determined. The coefficients of variation and 95 percent confidence limits of the deviations from test data are evaluated. It is found that the proposed model is more representative of actual conditions than previous methods.

Improvements of prediction when measurements of short-time deformation are available are also discussed. Finally, a detailed practical example of a segmental box girder bridge is given.

Deformations due to creep and shrinkage are normally several times larger than elastic deformations in concrete structures. Frequently, these deformations cause excessive cracking and deflections or possible failure with an inherent loss in serviceability, durability and long-time safety of concrete structures. Thus, there is an urgent need for a reliable method to predict creep and shrinkage, especially for slender prestressed concrete structures.

Recently, we have witnessed efforts to introduce creep and shrinkage into design recommendations[1,2,3] and to develop more realistic prediction formulas.[4] Over the last decade, however, the subject has been plagued by persistent disagreement as to what is the proper and optimal formulation to be used.[5-8] Although several pertinent conclusions have been drawn from theoretical arguments,[5-8] we shall deliberately leave them out. The most relevant and convincing argument is, of course, the experimental evidence and how well the data correlate with the actual behavior of existing structures.

Although this has not been generally realized, vast experimental information on creep and shrinkage has already been accumulated in the literature.[4] Unfortunately, the provisions of a recent international model code were supported by very limited comparisons with test data, selected somewhat arbitrarily. This was understandable in view of the tediousness of test data fitting when performed in the traditional way—by hand. Recently, however, highly effective computer optimization methods for analyzing and fitting test data have been developed[5,6] and, at the same time, the available test data from various laboratories have been collected and organized.[4]

This enabled development of a new prediction model in Reference 4 which we will call the BP model. Compared to other existing models,[1,2,3] this one gives a far superior overall agreement with the bulk of available test data[4] (80 different data sets). The coefficient of variation of the creep prediction is as low as 8 to 12 percent when the elastic modulus or one shrinkage value is known, and about 16 to 24 percent when it is unknown.

To attain good accuracy, the earlier BP model[4] requires that not only the strength but also several composition (mix) parameters of concrete be known. Branson's (ACI 209)[2,3] model is similarly based. On the other hand, the input for the CEB-FIP Model Code formulation[1] is more limited, requiring only the strength and the type of cement, and possibly the elastic modulus of concrete. For preliminary design, in which the composition of the concrete to be used might not yet be known, and also for the design of ordinary structures, it is desirable to have a simpler model that requires as few material characteristics as possible, preferably just the strength, while maintaining at the same time a sufficient accuracy.

Development of such a model, which we will call BP2, is our main objective. This model will represent a simplified version of the earlier BP model;[4] hence, the background discussions[4,9-11] need not be repeated. Although an accurate prediction of creep and shrinkage is needed mainly for prestressed structures, the model can of course be used for all concrete structures.

To estimate the error in material description, we adopt as our second objective a statistical analysis of the deviations from test data. At the same time, we will compare the data fits for the present model with those of Branson's (ACI) model[2,3] and the CEB-FIP Model Code.[1] In the process these two will be also compared mutually; this has not been done previously, in spite of much discussion. For a comparison of the previous BP model with the same and many further test data, Reference 4 may be consulted.

*Formerly, Graduate Research Assistant, Northwestern University, Evanston, Illinois.

Proposed Model

The essential structure of our model, which distinguishes it from the ACI,[2,3] CEB-FIP,[1] and other formulations, is as follows:
Shrinkage strain:

$$\epsilon_{sh} = \epsilon_{sh\infty} k_h S\left(\frac{\hat{t}}{\tau_{sh}}\right), \quad \hat{t} = t - t_o \quad (1)$$

Strain due to unit stress:

$$\epsilon = J(t,t') = \underbrace{\frac{1}{E_0}}_{\text{instant}} + \underbrace{A(t')F(\bar{t})}_{\text{basic creep}} + \underbrace{k_h' P(\Delta_d) B(t') f\left(\frac{\hat{t}}{\tau_{sh}}\right)}_{\text{drying creep}} \quad (2)$$

where

$J(t,t')$ = creep (compliance) function[34] = strain at time t (in days) caused by a unit uniaxial stress sustained since time t' (in days)
$\bar{t} = t - t'$ = stress duration
$\Delta_d = t' - t_o$ = lag of the instant of loading t' after the start of drying
$\hat{t}$ = drying duration
k_h and k_h' = functions of ambient humidity
τ_{sh} = shrinkage-square halftime which is proportional to the size square

Note that S, A, F, P, B, and f are functions of the indicated variables.

There are no humidity and size effects in the basic creep term; these effects appear only in the drying creep term. A change of humidity is manifested by a vertical scaling of this term, and a change in size (thickness) causes in the log-time plots a horizontal shift of the drying creep term,[42] which can be imagined to slide on top of the basic creep curve depending on the value of τ_{sh}. The presence of the shrinkage-like function $f(\hat{t}/\tau_{sh})$ in Eq. (2) means that shrinkage and creep are not assumed to be simply additive, which agrees with experimental evidence. (The relative differences with respect to other creep laws are discussed in Reference 42.)

Shrinkage

We use[4] the hyperbolic law in time and the cubic humidity dependence:

$$S\left(\frac{\hat{t}}{\tau_{sh}}\right) = \sqrt{\frac{\hat{t}}{\tau_{sh} + \hat{t}}} \quad (3)$$

$$k_h = 1 - h^3 \text{ for } h \leq 0.98; \quad (4a)$$

$$k_h = -0.2 \text{ for } h = 1.00 \quad (4b)$$

For the effects of size, diffusivity and age, the earlier BP formulas[4] are simplified as:

$$\tau_{sh} = \frac{(k_S D)^2}{C_1(t_0)}; \quad D = 2\frac{v}{s};$$

$$C_1(t_0) = 2.4 + \frac{120}{\sqrt{t_0}} \quad (5)$$

in which

t = time (in days), representing the age of concrete
t_0 = age when drying begins
$\hat{t}$ = duration of drying
ϵ_{sh} = shrinkage strain
$\epsilon_{sh\infty}$ = ultimate shrinkage
h = relative humidity of the environment
τ_{sh} = shrinkage square halftime
$C_1(t_0)$ = coefficient proportional to drying diffusivity at age t_0
D = effective cross section thickness in mm
v/s = volume-to-surface ratio in mm
k_S = shape factor which equals 1.0 for a slab, 1.15 for a cylinder, 1.25 for a square prism, 1.30 for a sphere, 1.55 for a cube (see Reference 11 which is based on Reference 12)

These formulas are deduced from the BP model by omitting the temperature dependence and the relatively small influence of the increase of elastic modulus with time. The fact that all shrinkage curves as functions of $\hat{t}/\tau_{sh}$ are proportional, and that τ_{sh} is proportional to D^2, k_S and to $1/C_1$, follow from nonlinear diffusion theory.[9,12] The remaining aspects are empirical. For a detailed analysis, see References 9 and 12.

Previously, both $C_1(t_0)$ and $\epsilon_{sh\infty}$ were derived as functions of the composition of concrete.[4] It has now been found that no large error is caused by omitting the composition dependence of $C_1(t_0)$, but for $\epsilon_{sh\infty}$ this turns out to be impossible without introducing errors over ±50 percent. It simply is not feasible to predict all properties of concrete without knowing its composition. For shrinkage, even a very crude guess of composition parameters is far better than none. Therefore, the composition formula from Reference 4 must be retained, except for removing the influence of elastic modulus; hence:

$$\epsilon_{sh\infty} = (1330 - 970y)10^{-6} \quad (6a)$$

$$y = (390z^{-4} + 1)^{-1} \quad (6b)$$

$$z = \sqrt{f_c'}\left[1.25\sqrt{\frac{a}{c}} + 0.5\left(\frac{g}{s}\right)^2\right] \times \left(\frac{1 + s/c}{w/c}\right)^{1/3} - 12$$

$$\text{if } z \geq 0, \text{ otherwise } z = 0 \quad (7)$$

where

f_c' = standard 28-day cylinder strength in ksi (1 ksi = 6.895 N/mm²)
w/c = water-cement ratio
a/c = aggregate-cement ratio
g/s = gravel-sand ratio (all by weight)

Sand is the aggregate passing sieve No. 4 (4.7 mm), and gravel is the rest. For an analysis and justification of Eq. (7), see Reference 4.

The verification of the above (BP2) formulas by the well documented shrinkage test data available in the literature[13-16] is shown in Figs. 1 and 2. The basic information on these data is summarized in Reference 4. The fits are good but not as close as those with the BP model.[4]

Basic Creep

This is the creep in the absence of moisture exchange. It is measured on sealed specimens and is pertinent to mass concrete as well as to the core of more massive cross sections. The creep under water is almost the same. The double power law,[5,9,10] used in the BP model, is simple enough to be retained:

$$J(t,t') = \frac{1}{E_0} + C_0(t,t') \quad (8a)$$

$$C_0(t,t') = \frac{\varphi_1}{E_0}(t'^{-m} + \alpha)(t - t')^n \quad (8b)$$

where E_0 is the asymptotic modulus.[4]

The expressions given for parameters m, n, α, φ_1 and E_0 give the value of the conventional static elastic modulus E (roughly in accordance with the ACI formula for calculating E from f_c') as $E = 1/J$ when $t - t' = 0.1$ day is substituted. The formulas even give the value of dynamic modulus E_{dyn} as $1/J$ when $t - t' = 10^{-7}$ day is substituted, and the age dependence of E

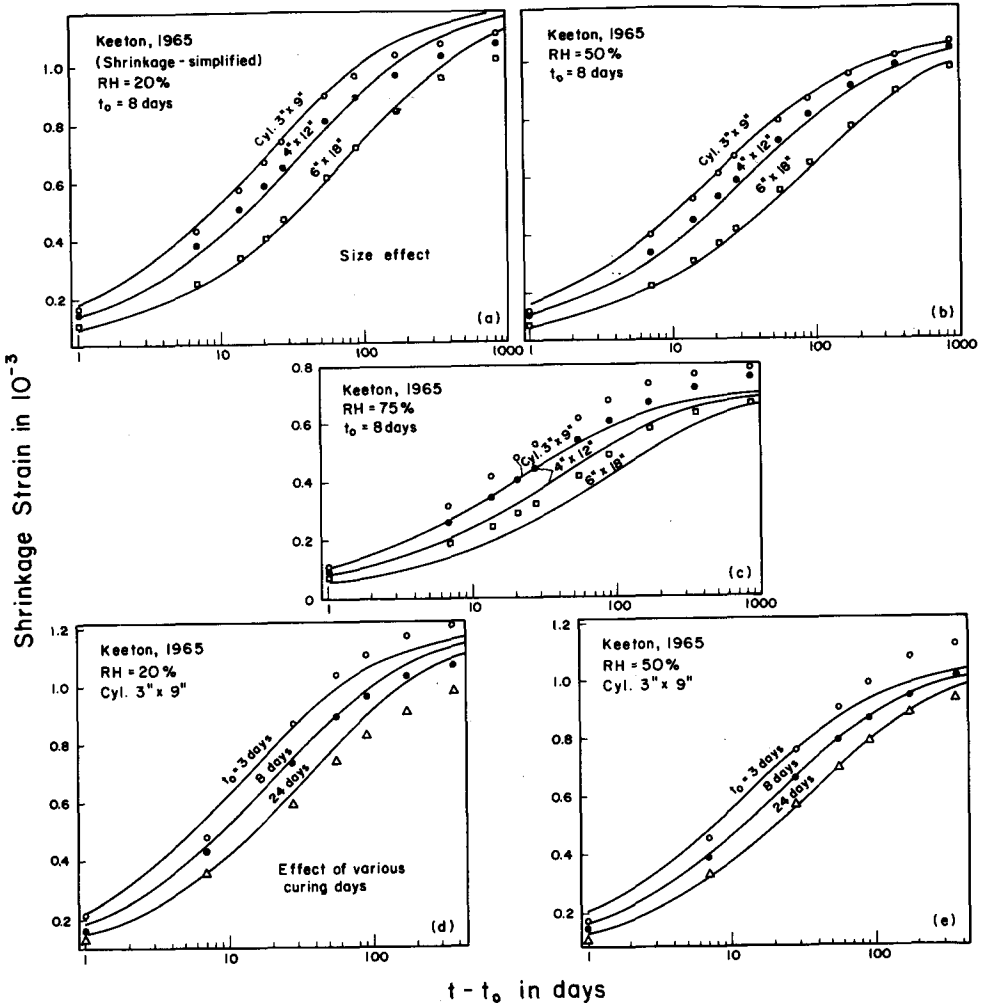

Fig. 1. Comparison of proposed model with shrinkage data.[16]

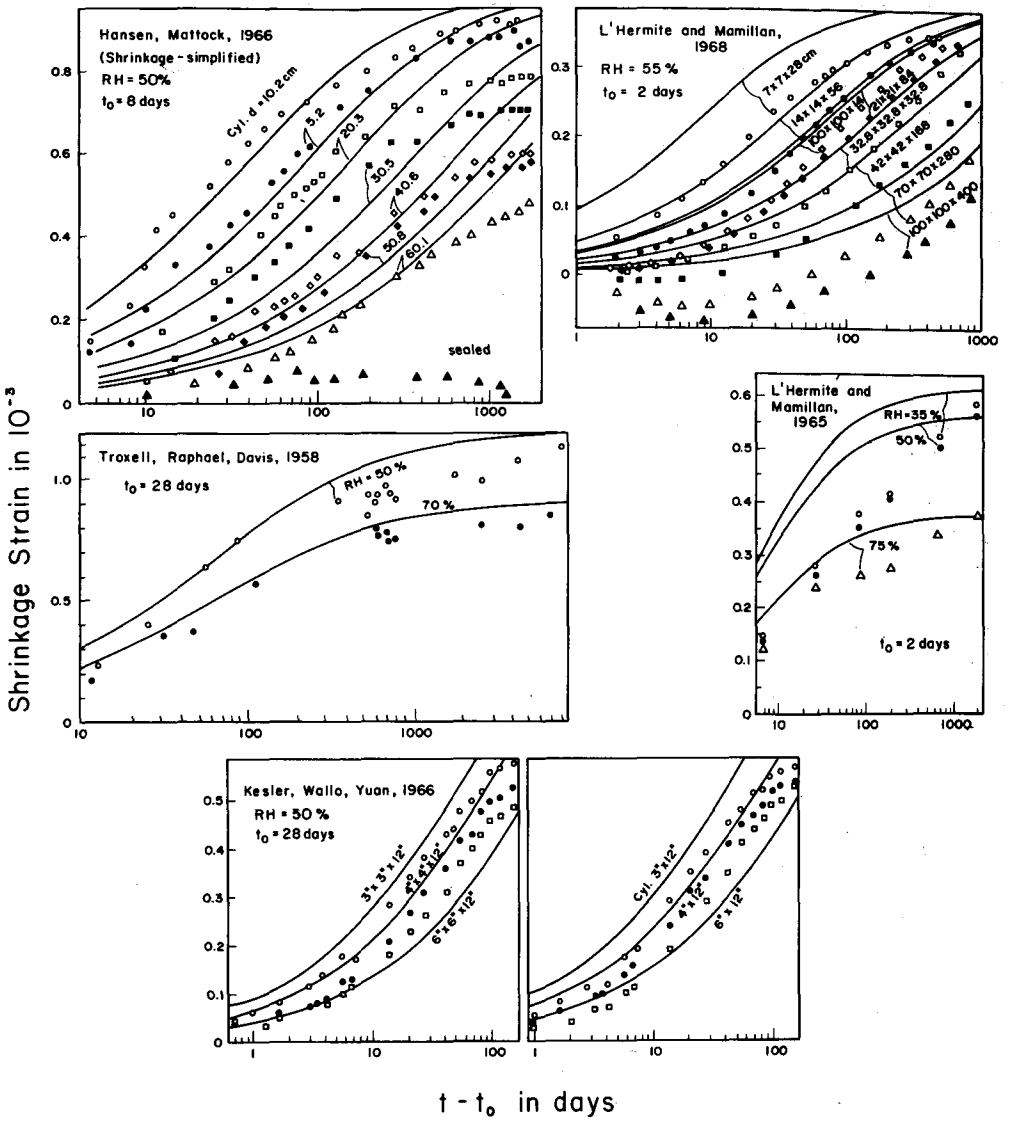

Fig. 2. Comparison of proposed model with further published shrinkage data.[4,13-15]

and E_{dyn}. However, to achieve simplification, we restrict this broad range of applicability because it is not needed for normal creep structural analysis.

The following simplified formulas, applicable to normal weight and normal strength concretes for load durations $t - t' \geq 1$ day, have been identified:

$$1/E_0 = 0.1 + 0.5/(f'_c)^2 \quad (9a)$$

$$\varphi_1 = 0.3 + 15\,(f'_c)^{-1.2} \quad (9b)$$

$$m = 0.28 + 1/(f'_c)^2 \quad (9c)$$

$$n = 0.115 + 0.0002\,(f'_c)^3 \quad (9d)$$

$$\alpha = 0.05 \quad (9e)$$

where f'_c is in ksi and $1/E_0$ is in 10^{-6}/psi.

Because of the afore-mentioned simplification, the approximate conventional elastic modulus at any age t' is obtained from these formulas as $E = 1/J$ for $t - t' = 1$ day, rather than 0.1 day. It should be also mentioned that slightly different formulas, namely:

$$1/E_0 = 0.09 + 0.465/(f'_c)^2$$

and

$$n = 0.115 + 0.00013\,(f'_c)^{3.4}$$

had been used in fitting the data in figures, and were later modified to Eq. (9) in order to extend the validity to relatively high f'_c and very long times beyond the range of test data in the figures.

The fits of the available well documented test data[17,26] are dis-

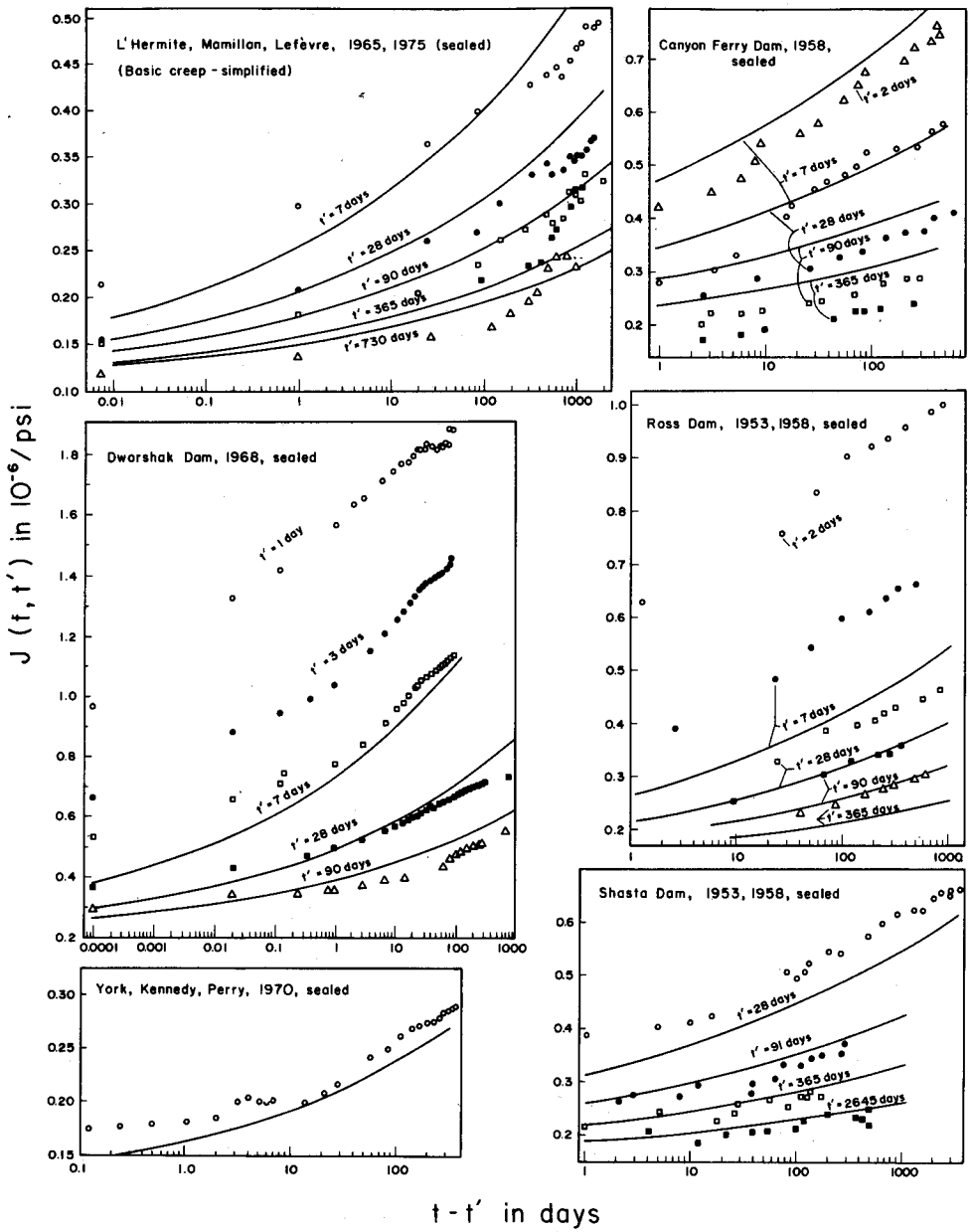

Fig. 3. Comparison of proposed model with published data on basic creep.[4,14,17-20,26]

played in Figs. 3 and 4 (and basic information on test data used can again be found in Fig. 4). Understandably, the fits are not as close as those with the BP model.[4]

Drying Creep

Simultaneous drying intensifies creep. This may be described by superimposing on the basic creep expression a shrinkage-like term, C_d

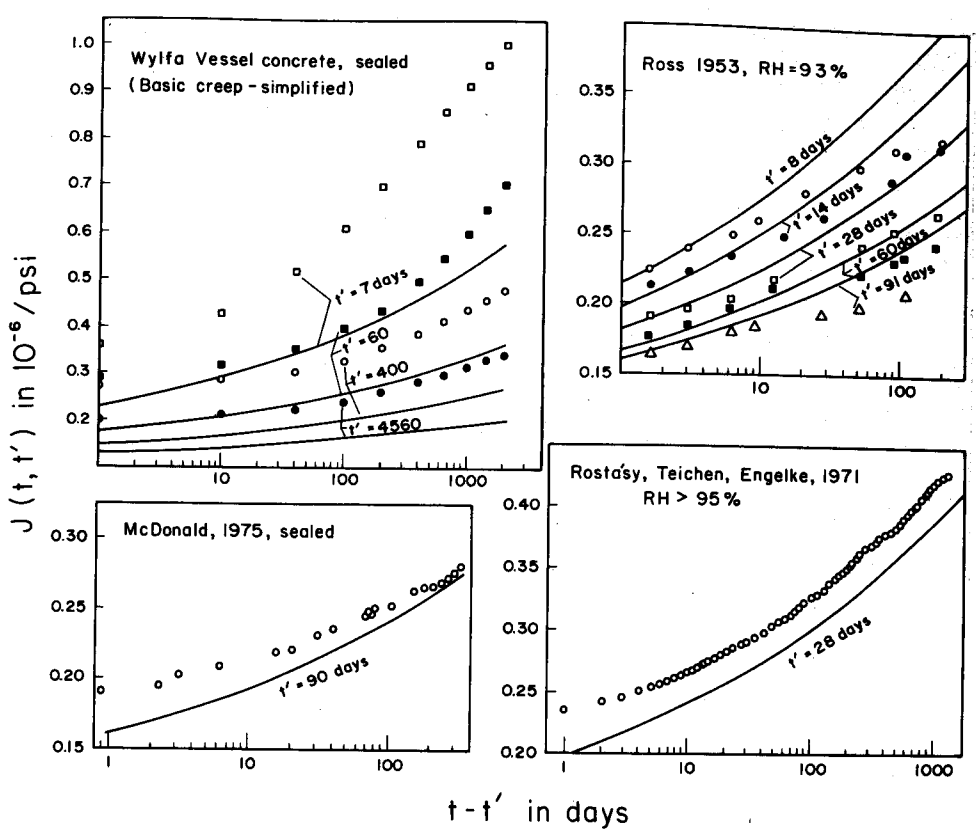

Fig. 4. Comparison of proposed model with further published data on basic creep.[2,21-25]

(t,t',t_0), where t' is the age at loading and t_0 is the age at the start of drying:[4,11]

$$J(t,t') = \frac{1}{E_0} + C_0(t,t') + C_d(t,t',t_0) \tag{10}$$

The effects of humidity and size enter only through the additional, drying creep term. The full model in Reference 4 involves another additive term, $-C_p(t,t',t_0)$, which models the decrease of creep that takes place long after the drying terminates. This term is omitted here, which means that our simplified model cannot describe the test data for predried specimens.

This omission precludes application of the formula to long creep times for very thin structures, such as thin shells, but for most other structures this does not matter because their drying reaches the stage of moisture equilibrium in the micropores long after their design lifetime.

By simplifying the expression of the BP model,[4] the following expression has been obtained:

$$C_d(t,t',t_0) = \frac{\tilde{\varphi}_d}{E_0} k_h' t'^{-m/2} S_d(t,t') \tag{11}$$

in which the humidity effect and the effect of the time lag of loading after the start of drying are given by:

$$k_h' = 1 - h^{1.5} \tag{12a}$$

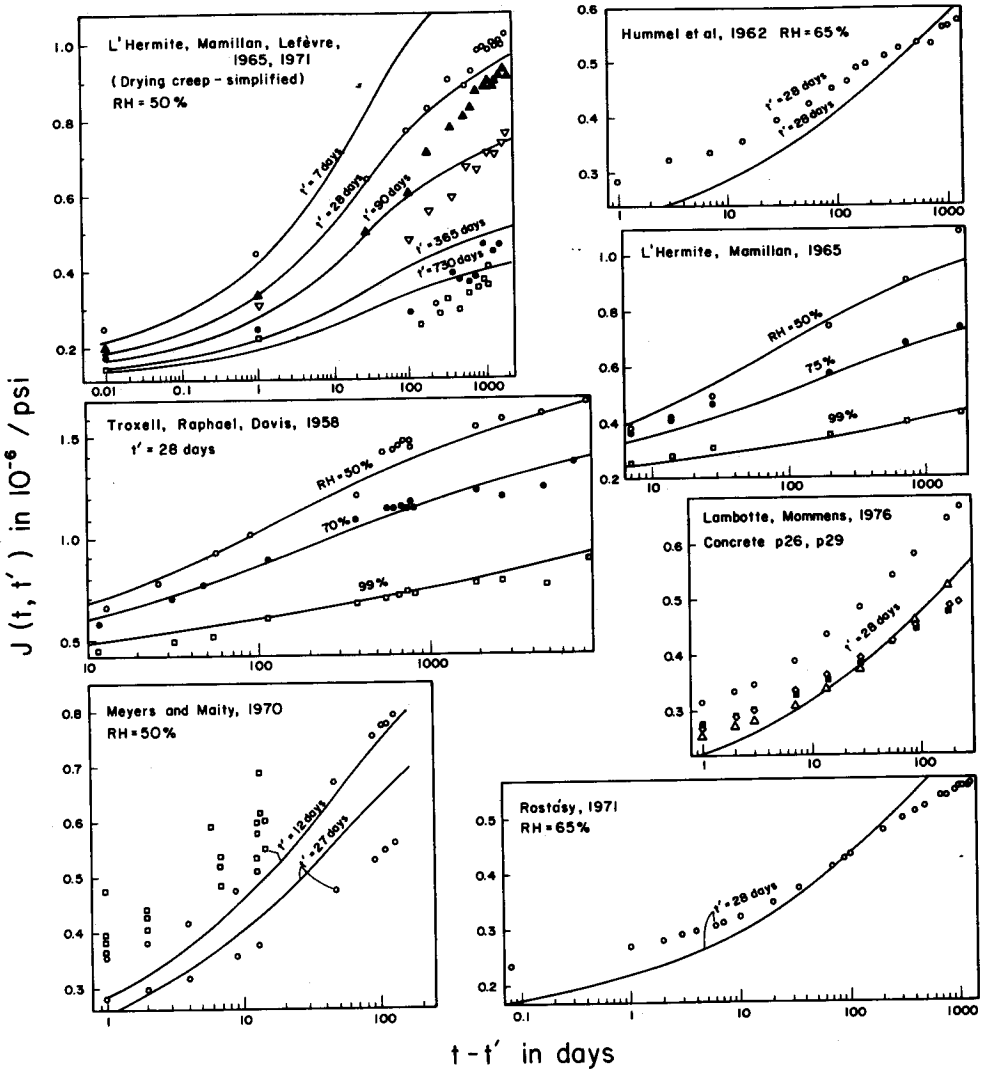

Fig. 5. Comparison of proposed model with published data on creep at drying.[4,14,15,17,24,28,29]

$$\bar{\varphi}_d = \left(1 + \frac{t' - t_0}{10\tau_{sh}} \right)^{-\frac{1}{2}} \varphi_d \left(10^6 \epsilon_{sh_\infty}\right) \tag{12b}$$

and the time evolution of the shrinkage-like term is:

$$S_d(t,t') = \left(1 + \frac{3\tau_{sh}}{t - t'} \right)^{-0.35} \tag{13}$$

where τ_{sh} involves the dependence on size and on diffusivity as a function of age [Eq. (5)], as indicated by the nonlinear diffusion theory. A detailed discussion of the individual terms of Eqs. (9) to (13) can be found in References 4 and 11.

Since the use of composition parameters is found to be inevitable for shrinkage, it would be inappropriate to discard the same composition pa-

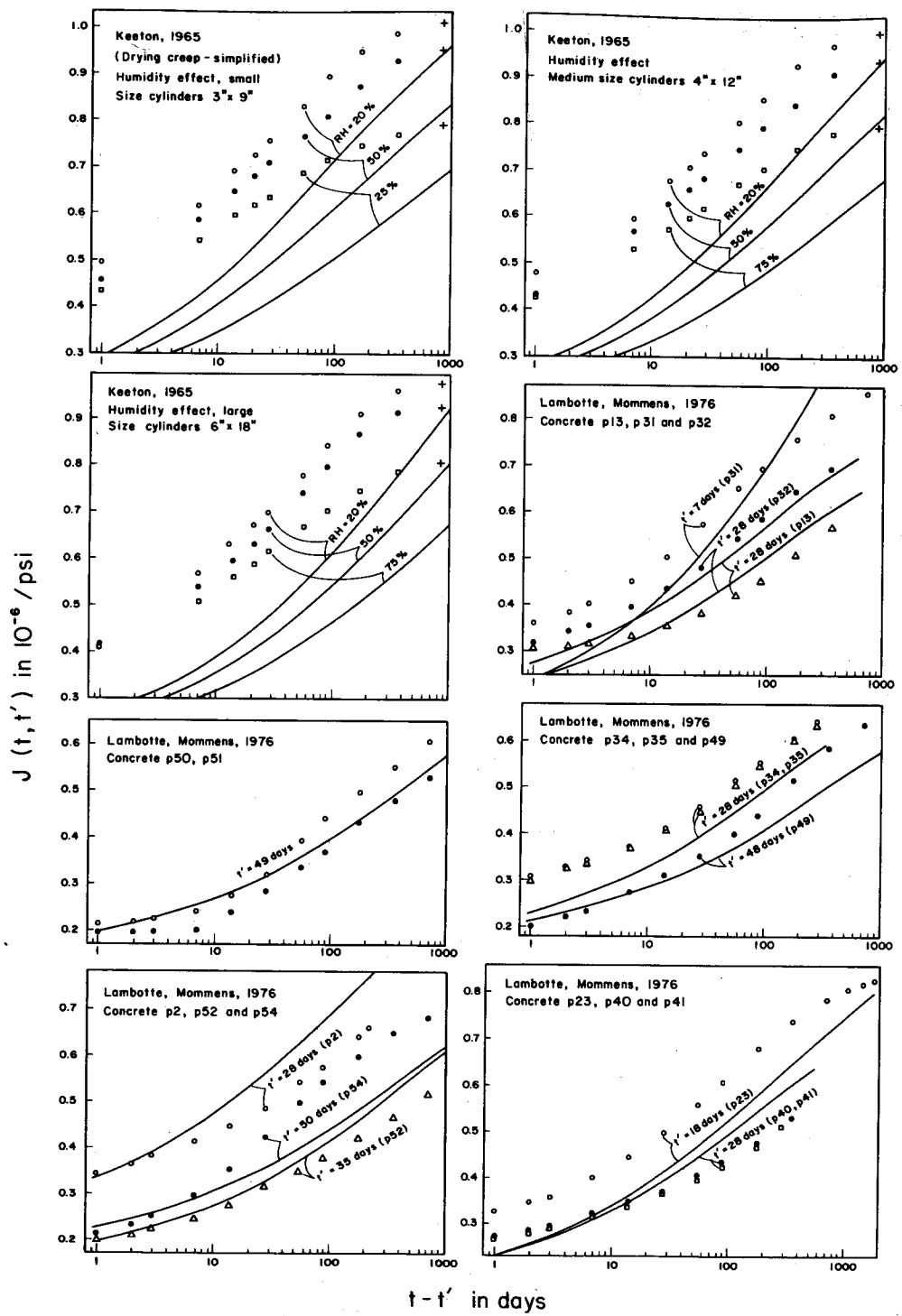

Fig. 6. Comparison of proposed model with further published data on creep at drying.[16,27]

rameters for drying creep, and it would certainly introduce a significant error. However, at least a simplified composition dependence has been identified:

$$r = \left(\frac{s}{a} f_c'\right)^{0.3} \left(\frac{g}{s}\right)^{1.3} \times \left(0.00161 \frac{w/c}{\epsilon_{sh_\infty}}\right)^{1.5} - 0.85 \quad (14a)$$

$$\text{for } r > 0: \varphi_d = 0.0056 + \frac{0.0189}{1 + 0.7r^{-1.4}}; \quad \text{otherwise } \varphi_d = 0.0056 \quad (14b)$$

In Eq. (14a) f_c' must be in ksi.

The fits of the most important test data[15-17,23,25] achieved with these formulas are shown in Figs. 5 and 6, and basic information on the test data used can again be found in Reference 4. The fits are clearly not as good as those with the BP model.[4]

Temperature and Cyclic Loading

These effects are normally neglected in the design of ordinary structures. It is preferable, though, to include them; the formulas from Reference 4, which do not involve any further composition effects, may be used.

Comparison with CEB and ACI Models

With the help of computer optimization of data fits, the solid curves shown in Fig. 1 through 6 have been obtained for the proposed model. The agreement with test data appears to be satisfactory. For comparison, the predictions of the CEB-FIP Model Code 1978[1] and of Branson's (ACI 209) Model[3,2] are matched against the same test data in Figs. 7-11. It is seen that the proposed (BP2) model gives clearly superior accuracy. (Comparisons with all data sets from Reference 4 have been considered but not all can be displayed here.)

Looking at Reference 4, we see that the previous BP model gives the best accuracy for the same data as displayed here. Furthermore, it closely fits the test data on other effects which are beyond the scope of the ACI and CEB models (such as short-time creep, very long time creep, creep after drying, temperature, and cyclic loading).

To make a quantitative comparison, the deviations of the prediction curves from the measured data have been evaluated at characteristic time points, taken as uniformly spaced points in log-time scales of $t - t'$ and $t - t_0$, two points per decade. From these deviations, the coefficients of variation ω for all data sets combined have been evaluated. For the designer, more meaningful parameters are the 95 percent confidence limits ω_5. In Reference 4 and here, the confidence limits referred to are one-sided 95 percent limits, i.e., the probability of exceeding the limit is 5 percent on the plus side, and also 5 percent on the minus side. This corresponds to the more usual two-sided confidence limit of 90 percent. These limits are obtained as $\omega_5 = 1.645\omega$ and their values, calculated on the basis of numerous data sets, are given in Table 1(A). The coefficients of variation and confidence limits for individual data sets are listed in Table 2. The method of statistical analysis is described in detail in Part VI of Reference 4.

When judging the statistical comparison in Tables 1 and 2, it must be appreciated that it is strongly biased against very long creep durations $t - t'$ and higher ages at loading t'. This is because the available data points for medium creep durations and medium ages at loading are far more numerous, and because, in cal-

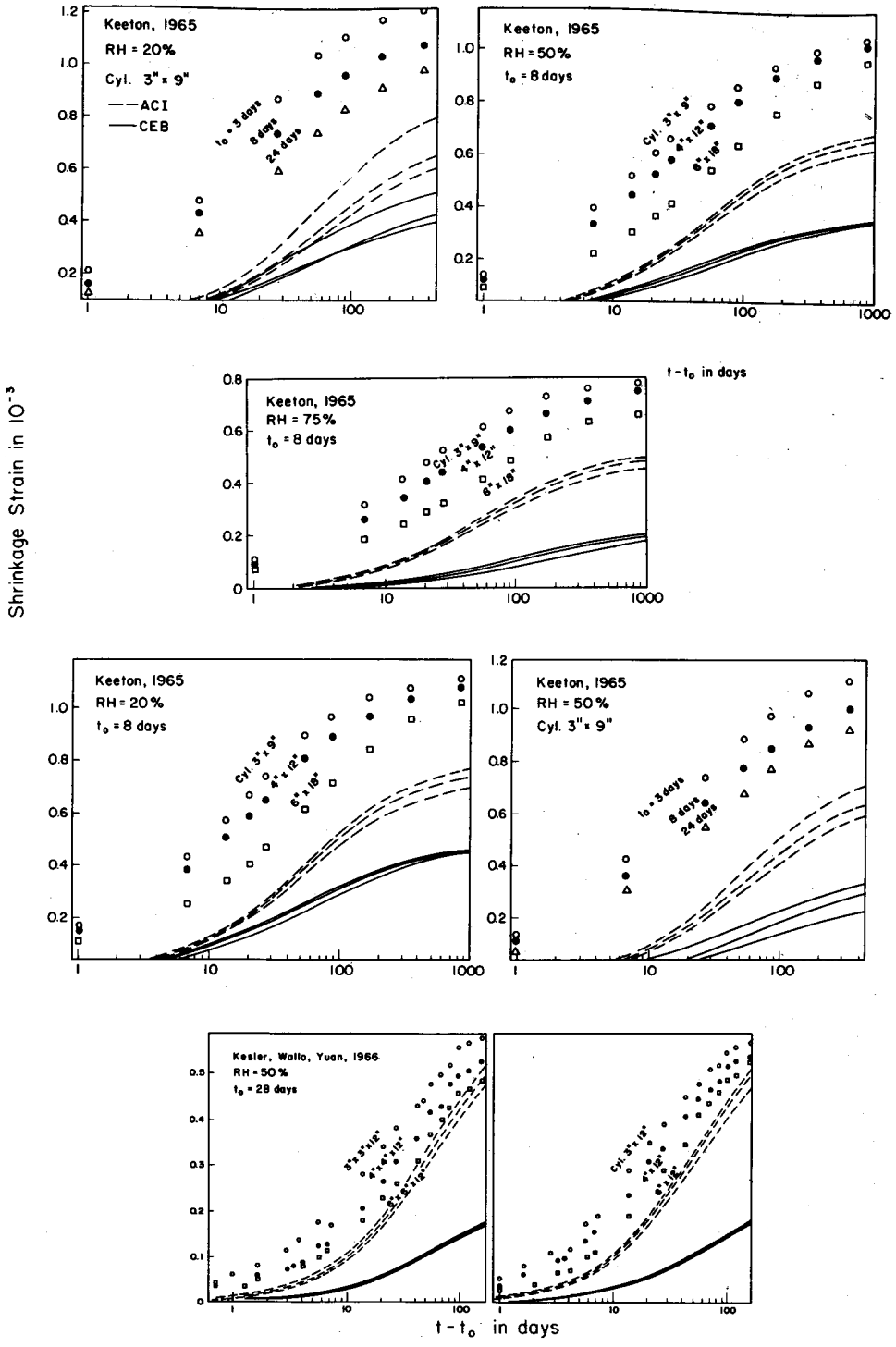

Fig. 7. Comparison of ACI and CEB models with published shrinkage data.[4,16]

Table 1. 95 percent confidence limits (in percent).

A. Comparison of various models

Model	Shrinkage	Basic creep	Drying creep	Overall
1. ACI 209 (1971)	86	52	42	63
2. CEB Model Code (1978)	118	47	32	76
3. Proposed BP2 model	37	45	29	37
4. BP Model (Ref. 4)	27	39	27	31
5. BP Model, one initial value given	22	13	16	18

B. Effect of selective use of test data on 95 percent confidence limits of BP model

Data set	Material parameters kept same	Parameters adjusted for best fit
1. Creep at room temperature:		
(a) All 36 data sets [a] (Ref. 4)	31.6	31.6
(b) Selected 25 best fitted data sets	22.5[b]	16[c,f]
(c) Selected 8 best fitted data sets	8.7[b]	7[c,f]
2. Shrinkage:		
(a) All 12 data sets [a] (Ref. 4)	52.2	52.2
(b) Selected 8 best fitted data sets	20.7	13[c,f]

C. Sources of error (95 percent confidence limits) in the BP model

Prediction model	Everything predicted	One value known	Each set fitted independently[d]	Error due to composition effects
(a) BP Model				
Shrinkage	27.1[e]	21.7	8[f]	19[f]
Basic creep	39.5	13.2	7[f]	32[f]
Drying creep	26.8	15.8	8[f]	19[f]
All combined	31.7	17.3	8[f]	24[f]
(b) Present BP2 Model (All)	38		10[f]	28[f]
(c) ACI 209 (All)	65		35[f]	30[f]
(d) CEB 78 (All)	75		40[f]	35[f]

[a] From Bažant-Panula, 1978-79.
[b] Material parameters kept the same as for all sets combined.
[c] Material parameters adjusted to give best fit for the selected data.
[d] This is the intrinsic error due to form of creep and shrinkage law.
[e] For 7 data sets; and 31.7 for 12 data sets (Ref. 4).
[f] Denotes very rough estimates.

culating Tables 1 and 2, the same weight has been given to all sampling points uniformly distributed in log-time scales (in order to avoid possible criticism of a subjective selection of uneven weights).

This bias works in favor of the ACI and CEB-FIP models rather than the BP and BP2 models whose broader scope (very long creep durations, high and very small ages at loading) is not adequately reflected in the values in Tables 1(A) and 2. Nevertheless, despite this bias, the proposed model still comes out superior.

Compared to the BP model, the proposed model overestimates the creep of very young concrete, although not as much as the ACI model, and its use therefore should be lim-

Table 2. Comparison of coefficients of variation (in percent) for individual data sets and various prediction models (biased against very long creep durations and high ages at loading).

Test data	BP Model El. Mod. or ϵ_{sh_∞} given[1]	(1978)[3] All by eqs.[2]	Proposed model	ACI (1971)	CEB (1978)
1. SHRINKAGE					
1. Hansen, Mattock	11.2	11.4	13.4	33.6	72.7
2. L'Hermite[6] 1968[4]	19.3	22.7	35.2	82.1	35.0
3. L'Hermite[6] 1965	14.6	23.6	35.1	34.8	21.6
4. Troxell[7] *et al.*	5.6	5.7	11.3	55.5	84.5
5. Kesler[8] *et al.*	16.2	20.6	22.5	30.5	93.3
6. Keeton—size	12.4	13.9	12.1	52.1	80.7
7. Keeton—age	7.9	8.3	8.5	59.1	81.9
$\bar{\omega} = (\Sigma\, \omega_i^2/7)^{\frac{1}{2}}$	13.2	16.5	22.4	52.5	71.7
(95% conf. limit)†	(21.7)	(27.1)	(36.8)	(86.4)	(117.9)
2. BASIC CREEP					
8. L'Hermite[6] *et al.*	8.1	25.2	8.9	52.3	19.8
9. Canyon Ferry[9]	8.0*	39.6*	45.4	47.3	18.7
10. Ross Dam[9]	15.6*	27.7*	25.1	16.3	25.5
11. Shasta Dam[9]	8.5	16.6	9.3	27.5	20.3
12. Dworshak Dam[10]	12.0	21.2	12.5	30.0	45.4
13. Wylfa Vessel[11]	9.4	21.0	46.0	35.4	46.0
14. A. D. Ross	4.3	33.7	13.1	35.0	14.2
15. York *et al.*[12]	3.6	16.1	9.0	23.2	8.7
16. Rostásy *et al.*	3.7	5.1	8.9	12.2	7.9
17. Keeton	3.3	26.9	49.2	36.4	52.4
18. McDonald	4.1	20.0	8.3	24.1	4.0
19. Maity, Meyers[14]	4.1	14.2	30.5	15.4	27.5
$\bar{\omega} = (\Sigma\, \omega_i^2/12)^{\frac{1}{2}}$	8.0	24.0	27.2	31.9	28.6
(95% conf. limit)†	(13.2)	(39.5)	(44.7)	(52.5)	(47.0)
3. DRYING CREEP					
20. L'Hermite[6], RH 50%	10.4	34.6	21.7	20.7	18.8
21. L'Hermite[6] 1965	15.9	3.7	8.0	25.6	9.8
22. Keeton	3.9	20.2	29.3	28.4	22.4
23. Troxell[7] *et al.*	5.9	8.6	4.4	31.3	27.5
24. Rostásy	5.3	6.1	17.1	8.0	16.9
25. Mossiossian[15]	14.3	6.2	23.3	31.7	15.6
26. Maity, Meyers[14]	5.9	17.4	14.7	35.3	27.0
27. Hummel *et al.*	36.2	6.5	12.8	10.3	16.3
28. Lambotte, Mommens[5]	12.0	16.9	15.8	24.6	16.0
$\bar{\omega} = (\Sigma\, \omega_i^2/9)^{\frac{1}{2}}$	9.6	16.3	17.8	25.6	19.7
(95% conf. limit)†	(15.8)	(26.8)	(29.3)	(42.1)	(32.4)
4. COMBINED SHRINKAGE, BASIC CREEP AND DRYING CREEP					
$\langle\omega\rangle = (\Sigma\, \bar{\omega}^2/3)^{\frac{1}{2}}$	10.5	19.3	22.8	38.4	46.0
(95% conf. limit)†	(17.3)	(31.7)	(37.5)	(63.2)	(75.7)

*Data for $t' = 2$ days included here but not for other columns, [1]modulus E_0 or ϵ_{s_∞} optimized or measured, [2]complete prediction, including elast. modulus, [3]Ref. 4, [4]where hydration heat caused expansion zero strain was assumed, [5]$(\Sigma\omega^2/12)^{\frac{1}{2}}$ for 12 tests: P2, P13, P23, P26-29, P31, P34-35, P40-41, P49, P50-51, P52 & P54, [6]with Mamillan, [7]with Raphael, Davis, [8]with Wallo, Juan, [9]Hanson, Harboe, [10]Pirtz, [11]Browne *et al.*, [12]with Kennedy, Perry, [14]Mixes A and B, [15]with Gamble.
†95% confidence limit in percent = 1.654 times the preceding line (for one-sided limit).

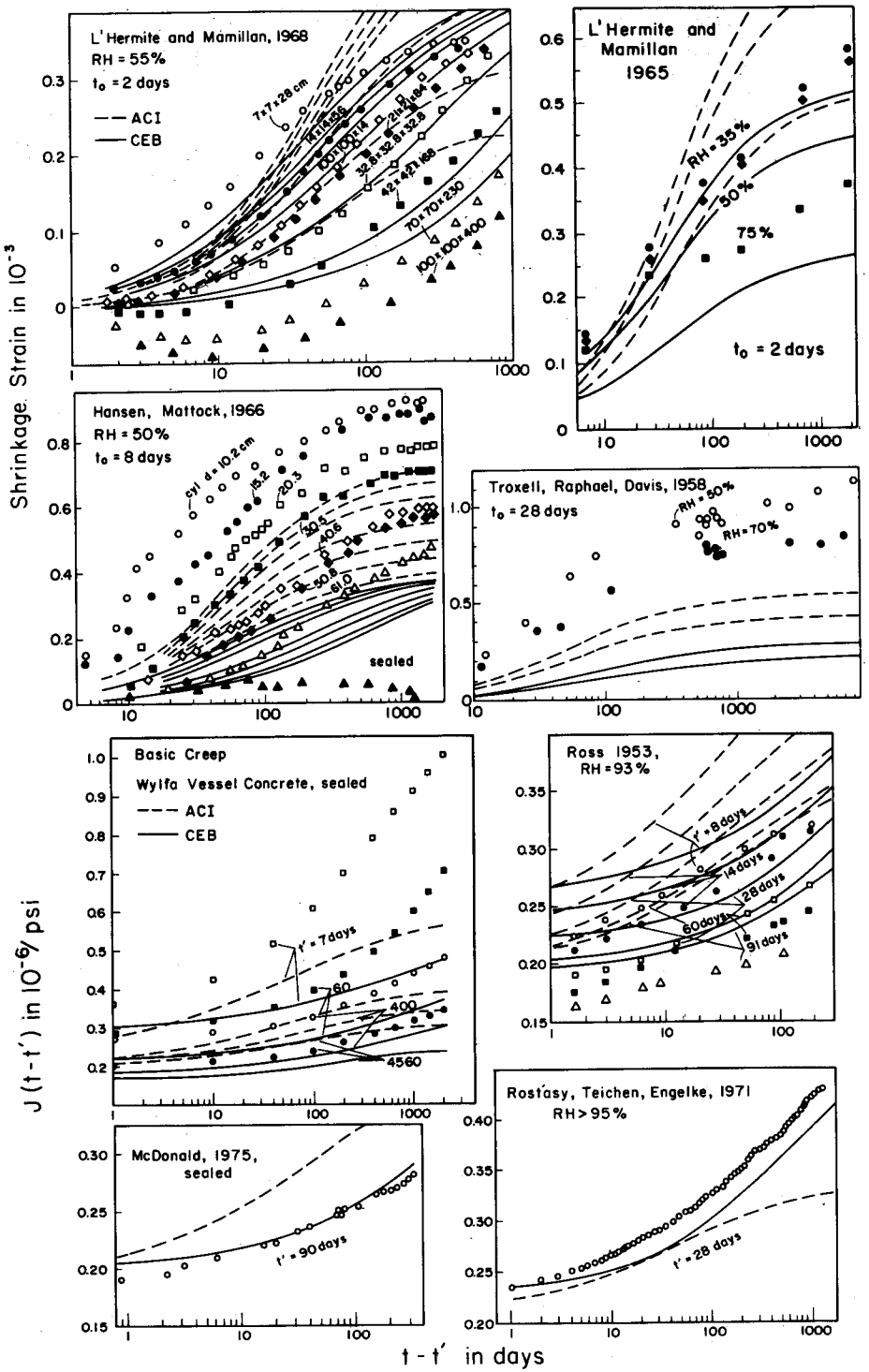

Fig. 8. Comparison of ACI and CEB models with further published shrinkage data[13-15,17] and with basic creep data.[4,21-25]

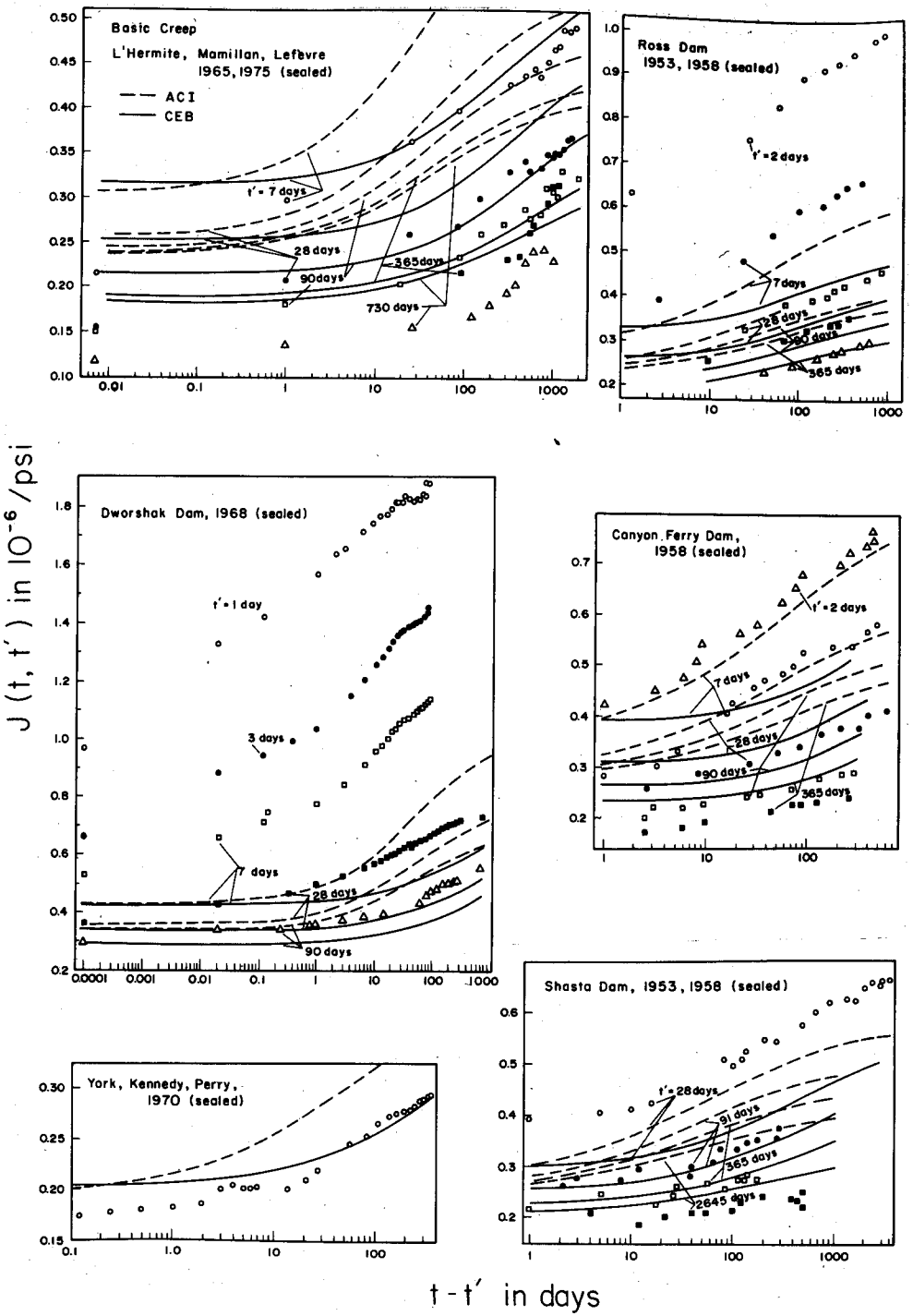

Fig. 9. Comparison of ACI and CEB models with further basic creep data.[4,14,17-20,26]

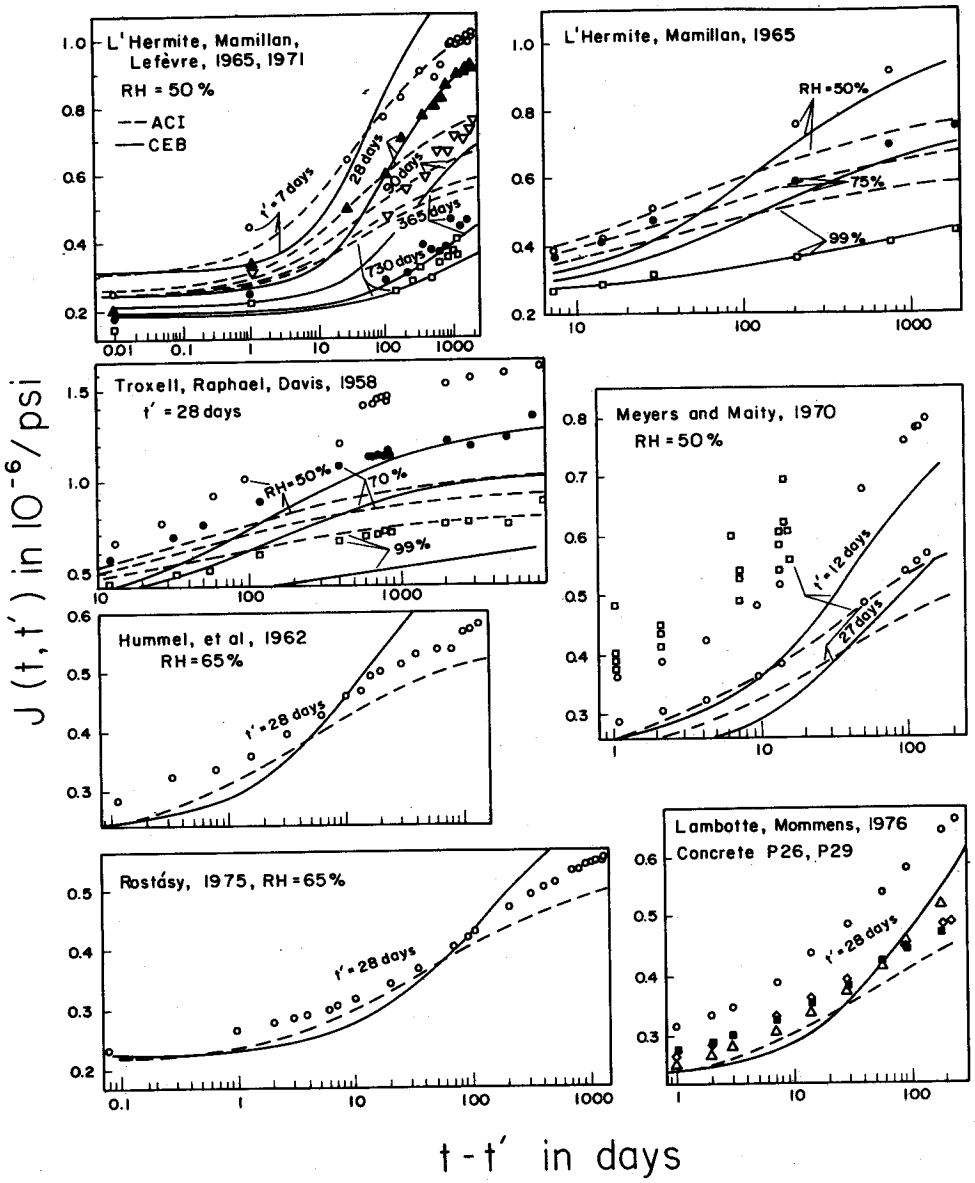

Fig. 10. Comparison of ACI and CEB models with published data on creep at drying.[14,15,17,24,27-29]

ited to loading ages $t' \geq 7$ days. The effect of the age at loading is generally more poorly represented in the CEB-FIP Model Code, and more poorly still in the ACI model; for these models, both the basic and drying creeps are much too high at high ages of loading. Even though the representation of drying creep at small loading ages is acceptable using the CEB-FIP Model Code, the effect of loading age upon drying creep is not

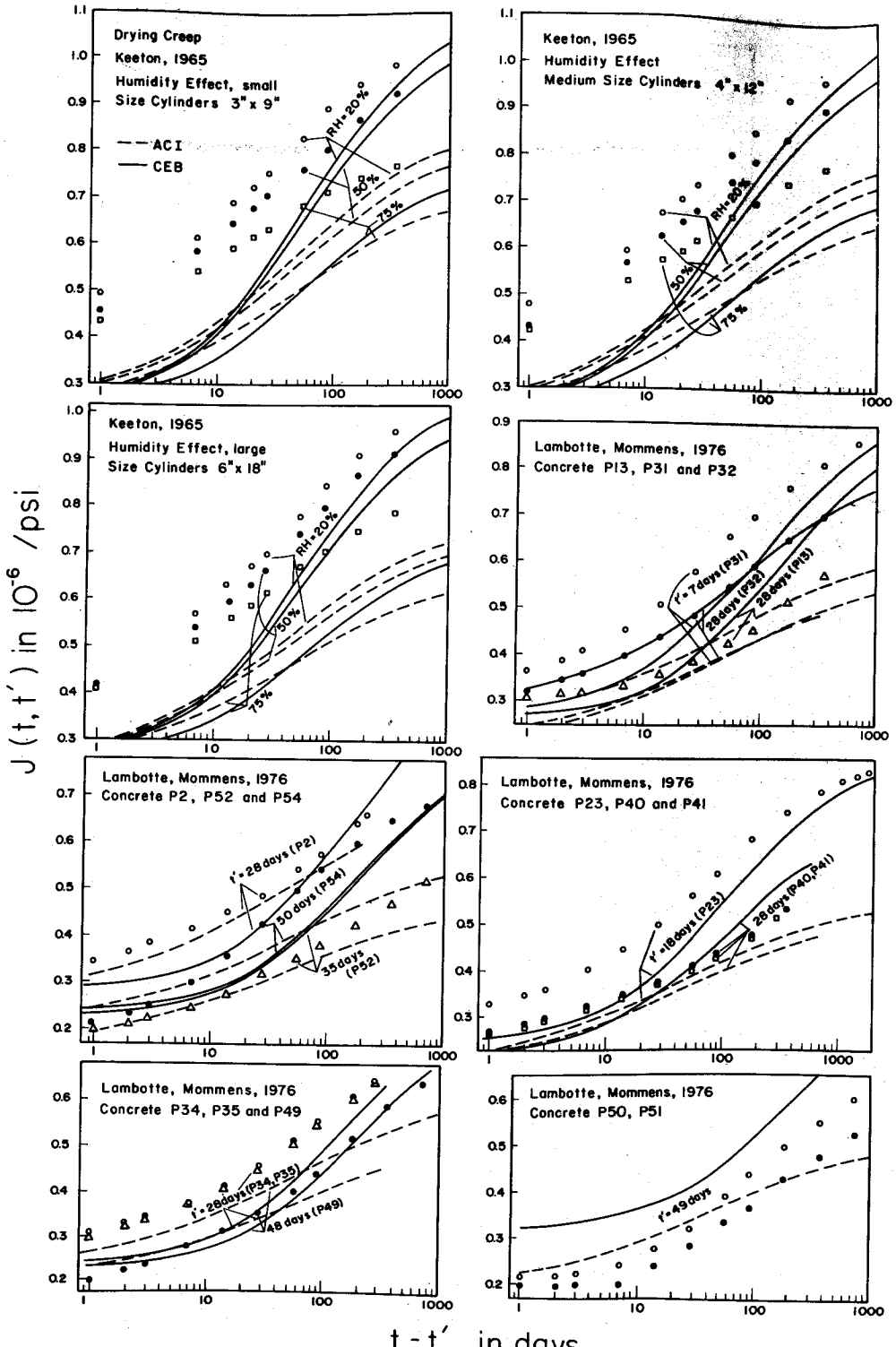

Fig. 11. Comparison of ACI and CEB models with published data on creep at drying.[16,27]

Table 3. Comparison of errors (95 percent confidence limits Δ_i) and laboriousness (man-hours, T_i) of structural analysis and creep prediction.

1. Error in structural analysis (internal force, displacement, max. stress) due to method of structural analysis alone[b]		
Method of structural analysis	T_1	Δ_1
A. Back of envelope calculation[a]	½h	25%
B. Stat. determinate simplification (portal method)	3h	10%
C. Simplified stat. indeterminate	6h	6%
D. Slope-deflection method, moment distribution, yield line th., etc.	20h	4%
E. Frame program, finite element program[e]	60h	2%

2. Error in structural analysis due to error in creep properties alone				
2a. Error in predicting creep properties as such			2b. Resulting error of structural analysis	
Method of creep prediction	T_2	Δ_2	b1. Creep sensitive problem[c] Δ_3	b2. Insensitive problem[d] Δ_4
(a) CCA 78[a]	¼h	75%	75%	8%
(b) CEB 78	2h	70%	70%	7%
(c) ACI 209	1h or ¼h[f]	65%	65%	7%
(d) BP2	2h	40%	40%	4%
(e) BP	3h or ¼h[f]	30%	30%	3%
(f) BP, initial value known	3h	18%	18%	2%

[a] 2-page formulation of Cement and Concrete Association, England, 1978.
[b] Assumes experienced analyst, no human error.
[c] For example, precast, simply supported beams made continuous; differential settlement; composite cross section; forces in midspan hinge of segmental bridge; creep buckling; shells.
[d] For example, stress distribution in a homogeneous frame, stresses in cracked cross section.
[e] Chiefly input preparation, output interpretation.
[f] If the creep prediction formulas are put on a computer.

well represented. The creep data which cover a wide range of loading ages (e.g., Wylfa Vessel concrete or Dworshak Dam concrete) are not predicted satisfactorily at all by the CEB and ACI models. The extremely large deviations, exhibited by these models in many cases, appear neither in the BP model nor in the proposed model (except that the Wylfa Vessel data are fitted poorly by the proposed model). The fits by the proposed model represent a compromise.

In comparison to the proposed model, the ACI and CEB models do not represent very well the overall trend of the creep curves and especially the basic creep curves; this, therefore, precludes the use of these models for extrapolating short-time creep data. At the beginning as well as at the end, the creep curves plotted in log-time scales are much too flat.

In the case of the ACI model,[2,3] based on the work of Branson *et al.*,[30-32] one is at least rewarded by simplicity. In fact, if for the sake of simplicity the curves for basic and drying creeps are chosen to have the same shape (i.e., to be mutually proportional), one cannot really do much better than the ACI model. But, this is not worth the penalty in error. Moreover, vertical scaling (multiplying by a constant factor) of the creep curves to account for the size effect, as used by the ACI model, is not realistic.

Rather, the change of size should be represented, according to the diffusion theory, by a horizontal shift of the additive drying creep term rather than by vertical scaling, and this procedure agrees with test results. Consequently, if vertical scaling is used, the long-time extrapolation of drying creep obtained for thin specimens is inevitably much too high, and for thick specimens much too low.

In general, the ACI and CEB models work better for drying creep than for basic creep. For the CEB Model Code in particular, the overall behavior within the available range of drying creep data is acceptable. (However, there exist too few drying creep data with loading ages outside the 28 to 90 days' range.) As for basic creep, the ACI curves lie generally too high, and so do the CEB-FIP curves, though to a lesser extent. The ACI model humidity dependence does not compare well with data; the difference between $h = 20$ and 50 percent is too small (see data of Keeton and L'Hermite *et al.*). For shrinkage, as opposed to creep, both the ACI and CEB models are especially far away from the data, while the proposed model is rather close. In the case of the CEB Model Code, this is partly due to the lack of composition (mix) factors, which confirms that the use of these factors is necessary for a good prediction of shrinkage.

The creep formulation from References 33 and 34, which has been used in the German Code DIN and also appeared in the preliminary version of the CEB-FIP Model Code,[35] was found in Reference 36 to be unsatisfactory and distinctly inferior in data fits to Branson's (ACI) model,[2,3] whereas the current CEB-FIP Model Code[1] predicts creep overall somewhat better than the ACI Model, although it is less simple. The substantial improvement is the result of modifications proposed in Reference 36 in order to compensate for the practice of "vertical shifting" of the creep curves[5] while displaying data fits. This improvement, which is based on a computer optimization of fits of many test data (summarized in Appendix A), has been subsequently adopted for the final CEB-FIP Model Code[1] (in which it however appears under a different name). By means of Figs. 7-11 and utilizing the values for basic and drying creeps in Table 1, we now demonstrate that this adopted modification of

References 33-35 does indeed bring about a rather significant improvement, mitigating part of the previous criticism.

Nevertheless, as we see from the figures and Tables 1 and 2, the CEB-FIP Model Code formulation[1] is still clearly inferior in data fits (confidence limits). It is also much more limited in scope than the BP model.[4] The procedure is not even simpler, although at first it might appear so because fewer formulas are used in the Model Code. This is partly because many functions are defined by graphs (16 curves). If all the curves were defined by equations, as in other models, the Model Code formulation would appear more complicated than the BP model. For computer programs, equations are of course clearly preferable to graphs. Formulas are also advantageous for predictions especially when using measured short-time values of creep.

In discussing the deviations from the experimental data, we should appreciate the importance of avoiding the subjective element in selecting the test data with which we compare our model. When we make a totally unbiased selection of test data (i.e., random, by casting a dice), the resulting error of course should not significantly depend on the number of data sets used (unless this number is too small, say six). However, any subjective judgment in selecting the data sets can be dangerously misleading. This is illustrated in Table 1(B). For example (see Reference 4), if among the 12 available shrinkage data sets[4] one selects the 8 best fitted data sets (which would certainly look to a casual reader as sufficient experimental verification), the confidence limit obtained from comparing our model to the test data drops from 52 to 21 percent and if one fits these 8 data sets independently of those which were left out, it drops to about 13 percent.[4] (It was for this reason that practically all test data which could be found in the literature were used in Reference 4.)

With regard to extensions beyond the range of available test data, theoretical and conceptual aspects are, of course, very important too. For their critical analysis, other works[5-7,9,10,41] are applicable.

Model Accuracy and Complexity

The fact that an increase in accuracy of prediction is inevitably accompanied by an increase in complexity of the model prompts us to ask: Is the increase in complexity worthwhile? The question must be viewed in context of the entire structural analysis process. The analysis of complex prestressed concrete structures is frequently performed by sophisticated methods (e.g., computer frame analysis, finite elements and elastoplastic methods), the error of which might be less than 2 percent, whereas the creep and shrinkage strains, which are several times larger than the elastic strains, are usually predicted by models whose error exceeds 65 percent with a 10 percent probability and is much larger than the error in strength. Such an approach makes little sense. Optimally, the effort spent on various tasks in the structural analysis process should be commensurate with the expected accuracy gain due to refinement of that task. A rough illustrative comparison of this type is attempted in Table 3. Although the precise values in this table may be disputed, they nevertheless give a general idea of the problem. It is apparent from this table that none of the existing methods for creep prediction is too complicated for all but creep-insensitive structures.

Errors Stemming from Creep Law and Composition Effects

What is the main source of error—is it the form of the creep and shrinkage laws or the material parameters involved?—Decidedly the latter. Table 1(C) shows that for our model the latter source causes about three-quarters of the total prediction error. The intrinsic error of the creep and shrinkage laws was determined by fitting the data set for each concrete independently of others, which was done in References 10 and 11. It is solely this type of experimental verification which should be used to judge whether the chosen form of creep and shrinkage law is good.[10,11] The BP and present models appear in such comparisons far superior to any other available model.[10,11]

If we do not determine the best material parameters for given concrete but predict them from strength and composition, the error increases. Unfortunately, this increase, which represents the error due to composition effects, is comparatively very large for all models [see Table 1(C)]. Despite much effort, our formulas for predicting the material parameters from composition are apparently not too good, and obviously there is much room for further research.

When the composition error is much larger than the intrinsic error of the creep law, as is true of our model in contrast to other models, a great improvement of prediction must result when even one short-time (or initial) value is measured. The improvement is found for our model to be indeed significant. For example, Reference 4 and Table 1(C) shows that the error drops on the average to one-third in basic creep and to two-thirds in drying environment. Note that for a creep law whose intrinsic form is not too realistic (theoretically unfounded, as in some other models), the improvement based on one measured value is relatively much less significant. It is here where the main advantage of the proposed model lies.

Prediction Improvement if a Short-Time Value is Known

The improvement on the basis of a measured short-time value can be achieved easily only if the creep and shrinkage laws are defined by formulas rather than graphs, and if these formulas can be inverted to allow a simple calculation of material parameters. The proposed model, like the BP model and unlike the CEB 78 model, makes this possible, as we will now demonstrate.

We should note that, to minimize the error, the measured short-time deformation value should be determined as an average from several specimens. Moreover, the average should be taken, if possible, only after the time curve of each specimen is smoothed in the vicinity of the chosen short time (e.g., 10 minutes, or 1 day).

Assume we know the value of $\epsilon_{sh}^{(0)}$, corresponding to some time $\hat{t}$ (not too short, though, $\hat{t} > \tau_{sh}/3$), time t_0, and some D, h and k_S. We may then proceed as follows:

First, calculate C_1, τ_{sh}, k_h, S from Eqs. (3) to (5).

Then, solve $\epsilon_{sh_\infty} = \epsilon_{sh}^{(0)}/k_h S$ from Eq. (1).

Now, using this value of ϵ_{sh_∞}, we can then calculate ϵ_{sh} for other values of $\hat{t}$, t_0, D, h and k_S, obtaining a far superior prediction, much better than that in Figs. 1 and 2. Obviously, by acquiring a single measured shrinkage value, we can disregard the composition parameters altogether.

Still closer predictions are possible if two shrinkage values $\epsilon_{sh}^{(1)}$ and $\epsilon_{sh}^{(2)}$ for two sufficiently different values $\hat{t}_{(1)}$, $\hat{t}_{(2)}$ (say $\hat{t}_{(2)} \geq 3\tau_{sh}$, $\hat{t}_{(1)} \approx \tau_{sh}/2$), and possibly also for two different $h_{(1)}$, $h_{(2)}$ and $D_{(1)}$, $D_{(2)}$, are measured. We then discard Eqs. (6) and (5) for ϵ_{sh_∞} and C_1 and calculate:

$$\frac{1}{C_t(t_0)} = \frac{\hat{t}_{(2)} - A\hat{t}_{(1)}}{A(k_S D_{(1)})^2 - (k_S D_{(2)})^2} \tag{15a}$$

$$A = \frac{\hat{t}_{(2)}}{\hat{t}_{(1)}}\left(\frac{\epsilon_{sh}^{(1)}}{\epsilon_{sh}^{(2)}}\frac{k_h}{k_h}^{(2)}_{(1)}\right)^2 \qquad (15b)$$

$$\tau_{sh}^{(1)} = \frac{k_s^2 D^2_{(1)}}{C_1(t_0)} \qquad (15c)$$

$$\tau_{sh}^{(2)} = \frac{k_S^2 D^2_{(2)}}{C_1(t_0)} \qquad (15d)$$

$$S_{(1)} = \sqrt{\frac{\hat{t}_{(1)}}{\tau_{sh}^{(1)} + \hat{t}_{(1)}}} \qquad (15e)$$

$$S_{(2)} = \sqrt{\frac{\hat{t}_{(2)}}{\tau_{sh}^{(2)} + \hat{t}_{(2)}}} \qquad (15f)$$

$$\epsilon_{sh_\infty} = \frac{\epsilon_{sh}^{(2)}}{k_h^{(2)} S_{(2)}} = \frac{\epsilon_{sh}^{(1)}}{k_h^{(1)} S_{(1)}} \qquad (15g)$$

From the above equations we can predict $\epsilon_{sh}(t,t_0)$ for any other case.

Basic Creep

If the elastic modulus or some short-time strain value is known, the prediction accuracy approximately triples.[4] Assume we know the value of the conventional static modulus, which is here obtained as J at $t - t' = \Delta t \approx 1$ day, i.e.,

$$E(t') = 1/J(t' + \Delta t, t')$$

The following procedure can then be used:

1. Evaluate φ_1, m, n and α from Eq. (9).
2. Substitute these values along with $J(t' + \Delta t, t') = 1/E(t')$. and $t - t' = \Delta t$ into Eq. (8) and solve for E_0:

$$E_o = E(t')[1 + \varphi_1(t'^{-m} + \alpha)\Delta t^n] \qquad (16)$$

where $\Delta t^n = 1^n = 1$.

3. Using this E_0 value instead of that found from Eq. (9), substantially better predictions of $J(t,t')$ at any t and t' can be obtained, much better than those in Figs. 3 and 4.

If we also measure one short-time creep value J_1, e.g., for $t - t' = t_2 = 14$ days, $t' = 28$ days, we further improve the prediction:

1. Calculate m, n and α from Eq. (9).
2. Write Eq. (8) twice, once for J at the aforementioned times, and once for $1/E$ as before; this yields a system of two linear equations for $1/E_0$ and φ_1/E_0:

$$\frac{1}{E_0} + (t'^{-m} + \alpha)\Delta t\frac{\varphi_1}{E_0} = \frac{1}{E} \qquad (17a)$$

$$\frac{1}{E_0} + (t'^{-m} + \alpha)t_2^n\ \frac{\varphi_1}{E_0} = J_1 \qquad (17b)$$

3. Solving $1/E_0$ and φ_1/E_0, we can then predict $J(t,t')$ for any t and t' from Eq. (8).

Other alternatives of course, are possible. For example:

1. Use Eq. (9) to get $1/E_0$, m and α.
2. Noting that $\log C_0 = n \log (t - t') + \log[(t'^{-m} + \alpha)\varphi_1/E_0]$, write this relation for $C_0 = (1/E) - (1/E_0)$ and for $C_0 = J_1 - 1/E_0$ (with $t - t' = t_2 = 14$ days):

$$n \log \Delta t + \log \frac{\varphi_1}{E_0} = \log\left(\frac{1}{E} - \frac{1}{E_0}\right) - \log(t'^{-m} + \alpha) \qquad (18a)$$

$$n \log t_2 + \log \frac{\varphi_1}{E_0} = \log\left(J_1 - \frac{1}{E_0}\right) - \log(t'^{-m} + \alpha) \qquad (18b)$$

which is a system of two linear equations for n and $\log(\varphi_1/E_0)$. Solving them, we can obtain n and φ_1/E_0, upon which we can predict $J(t,t')$ for any time t' and t from Eq. (8).

The latter prediction will normally differ somewhat from the previous one [Eq. (17)]. It may, however, be advisable to carry out both predictions to get an idea of the range to expect. Various other alternative procedures are possible, too, but they require solving transcendental equations.

Drying Creep

If we can measure the value of $J(t,t')$ for some relatively small $t - t'$ value (perhaps $t - t' \geq \tau_{sh}/10$) and certain parameters t', t_0, D, h, k_S, we can again greatly improve the accuracy:

1. Calculate E_0, φ_1, m, n and α from Eq. (9) and also k_h', $S_d(t,t')$ from Eqs. (12) and (13), and $C_0(t,t')$ from Eq. (8).
2. Then solve $C_d(t,t',t_0)$ for these t, t' and t_0 values from Eq. (10), and also solve the $\bar{\varphi}_d$ value from Eq. (11).
3. Now use this $\bar{\varphi}_d$ value, instead of φ_d from Eqs. (12) and (14), to calculate $J(t,t')$ for any other t, t', t_0, D, h and k_S, greatly improving the accuracy and at the same time eliminating the need for composition parameters.

Further accuracy is possible if we, in addition, have the experimental elastic modulus E (e.g., for $t - t' = 1$ day). Then we do not need to estimate E_0 from Eq. (9), as above, but instead we can calculate it from Eq. (8), as in case of basic creep. We then proceed using Steps 1, 2, 3 as described above.

It is interesting to note that by having some measurements we can disregard the composition parameters in the BP model.[4] For this, we need to know the measured values of: (1) shrinkage at two different times or thicknesses, (2) elastic modulus and one short-time basic creep value (for, say, $t - t' = 7$ days) to predict basic creep, and (3) elastic modulus and two creep values to predict drying creep.

It is also worth mentioning that, because graphs are employed rather than formulas, the CEB-FIP model becomes too cumbersome to use effectively when a measured short-time creep value or two shrinkage values are given.

Application—Prestressed Segmental Bridge

To illustrate the proposed method, let us calculate the long-time deflections and internal force redistributions due to dead load for a typical box girder bridge erected from precast segments by the cantilever method. To allow use of the same steel form and traveling scaffold, the erection of the second cantilever forming the span begins after the first one is completed.

We assume that the left cantilever (Fig. 12) is $t_a = 270$ days old and the right one is $t_b = 90$ days old when

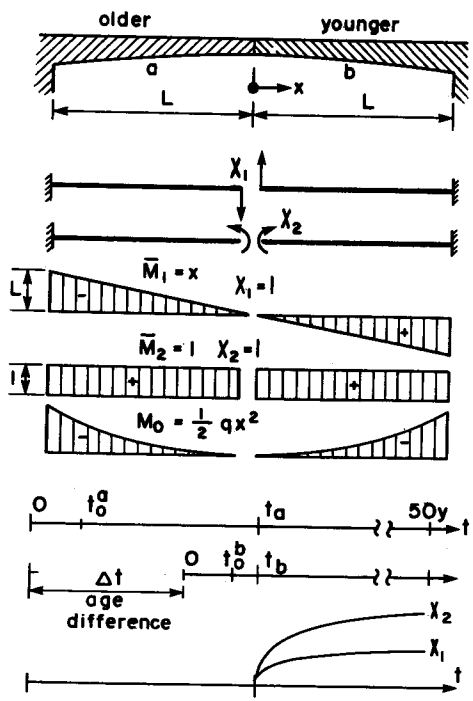

Fig. 12. Example of a segmental bridge.

they are joined at midspan. The joining is continuous or by a hinge. The cantilevers are connected without any jacking, and so the force in the joint is zero at the beginning. For simplicity we assume that both cantilevers are fixed at their ends.

Although our proposed method is applicable to varying ages of concrete along the span, we assume that within each cantilever the age is uniform in order to abbreviate the length of calculations. In practice, the dead weight increases gradually as the cantilevers grow, but for the sake of simplicity we consider that all dead weight is applied at once, when the concrete is $t' = 60$ days old. We further assume that the dead load is uniform with $q = 140$ kN/m.

Each cantilever is 48 m long (span = 96 m). The centroidal moments of inertia of the cross sections spaced at intervals $\Delta x = 12$ m, beginning at midspan, are $I = 2.52$, 4.27, 10.9, 28.3, and 64.2 m^4. (These values are taken from first author's design of the bridge over Vltava at Hladná, Czechoslovakia, in 1961.) We assume our bridge is built of concrete of 6000 psi (6 ksi) standard cylindrical strength, water-cement ratio 0.42, and sand-gravel-cement ratio 2.1:2.7:1. Let us now go to the detailed calculations.

From Eq. (7):

$$z = \sqrt{6}\left[1.25\sqrt{4.8} + 0.5\left(\frac{2.7}{2.1}\right)^2\right] \times \left[\frac{1+2.1}{0.42}\right]^{1/3} - 12 = 5.003$$

From Eq. (6):

$$y = (390 \times 5.003^{-4} + 1) = 0.616$$

$$\epsilon_{sh,\infty} = (1330 - 970 \times 0.616) \times 10^{-6} = 732 \times 10^{-6}$$

From Eq. (9):

$$1/E_o = (0.1 + 0.5/0.6^2) \times 10^{-6} \quad (19a)$$
$$= 0.1139 \times 10^{-6}/\text{psi}$$
$$\varphi_1 = 0.3 + 15/6^{1.2} = 2.047 \quad (19b)$$
$$m = 0.28 + 6^{-2} = 0.3078 \quad (19c)$$
$$n = 0.115 + 0.0002 \times 6^3 = 0.158 \quad (19d)$$
$$\alpha = 0.05 \quad (19e)$$

As for the effects of drying we will assume, again for the sake of simplicity, that all segments of the girder are 0.35 m thick ($D = 350$ mm, $k_S = 1$), drying on both surfaces in an environment of 65 percent relative humidity ($h = 0.65$), and that the exposure to the environment begins when the concrete is 7 days old ($t_o = 7$ days). From Eqs. (1) through (5):

$$C_1(t_o) = 2.4 + 120/\sqrt{7} = 47.76 \quad (20a)$$
$$k_h = 1 - 0.65^3 = 0.725 \quad (20b)$$
$$\tau_{sh} = (1 \times 350)^2/47.76 = 2565 \text{ days} \quad (20c)$$

The bridge is to be designed for the life span $t_l = 50$ years (i.e., 18263 days). Then:

$$\hat{t} = t_l - t_o = 18{,}263 - 7 = 18255 \text{ days}$$

and

$$S(\hat{t}) = (1 + 2565/18255)^{-\frac{1}{2}} = 0.9364 \quad (21a)$$

$$\epsilon_{sh}(t,t_o) = 732 \times 10^{-6} \times 0.7254 \times 0.9364 \quad (21b)$$
$$= 497 \times 10^{-6}$$

From Eq. (8):

$$E(60) = J(60+1, 60)^{-1} \quad (22a)$$
$$= \{0.1139[1 + 2.047(60^{-0.3078} + 0.05) \times 1^{0.158}]\}^{-1}$$
$$= 5.216 \times 10^6 \text{ psi}$$

$$E(90) = \{0.1139[1 + 2.047(90^{-0.3078} + 0.05) \times 1^{0.158}]\}^{-1} \quad (22b)$$
$$= 5.437 \times 10^6 \text{ psi}$$

$$E(270) = \{0.1139[1 + 2.047(270^{-0.3078} + 0.05) \times 1^{0.158}]\}^{-1} \quad (22c)$$
$$= 5.982 \times 10^6 \text{ psi}$$

Also from Eq. (8), the basic creep function values are:

$$J(18263,60) = 0.1139[1 + 0.6829] \times 18203^{0.158} \times 10^{-6}$$
$$= 0.4803 \times 10^{-6}/\text{psi} \quad (23a)$$

$$J(18083,60) = 0.1139[1 + 0.6829] \times 18023^{0.158} \times 10^{-6}$$
$$= 0.4797 \times 10^{-6}/\text{psi} \quad (23b)$$

$$J(90,60) = 0.1139[1 + 0.6829] \times 30^{0.158} \times 10^{-6}$$
$$= 0.247 \times 10^{-6}/\text{psi} \quad (23c)$$

$$J(270,60) = 0.1139[1 + 0.6829] \times 210^{0.158} \times 10^{-6}$$
$$= 0.294 \times 10^{-6}/\text{psi} \quad (23d)$$

where $0.6829 = 2.047(60^{-0.3078} + 0.05)$.

For the drying creep terms we get from Eqs. (12) and (13):

$$\bar{\varphi}_d = [1 + (60-7)/(10 \times 2565)]^{-\frac{1}{2}} \times 0.01521 \times 732 = 11.13$$

$$k_h' = 1 - 0.65^{1.5} = 0.476$$

$$S_d(18263,60) = [1 + (3 \times 2565)/(18263 - 60)]^{-0.35} = 0.8839 \quad (24a)$$

$$S_d(90,60) = [1 + (3 \times 2565)/(90 - 60)]^{-0.35} = 0.1433 \quad (24b)$$

$$S_d(270,60) = \ldots = 0.2809 \quad (24c)$$

$$S_d(18083,60) = 0.8830 \quad (24d)$$

Now from Eq. (11):

$$C_d(18263,60,7) = 11.13 \times 0.1139 \times 0.476 \times 60^{-0.3078/2} \times 0.8839 \times 10^{-6}$$
$$= 0.2817 \times 10^{-6} \quad (25a)$$

$$C_d(18083,60,7) = 0.3212 \times 0.8830 \times 10^{-6}$$
$$= 0.2836 \times 10^{-6} \quad (25b)$$

$$C_d(270,60,7) = 0.3212 \times 0.2809 \times 10^{-6}$$
$$= 0.0902 \times 10^{-6} \quad (25c)$$

$$C_d(90,60,7) = 0.3212 \times 0.1433 \times 10^{-6}$$
$$= 0.046 \times 10^{-6} \quad (25d)$$

This gives the total creep function values [Eq. (10)]:

$$J(18263,60) = (0.4803 + 0.2817) \times 10^{-6}$$
$$= 0.762 \times 10^{-6}/\text{psi} \quad (26a)$$

$$J(18083,60) = (0.4797 + 0.2836) \times 10^{-6}$$
$$= 0.763 \times 10^{-6}/\text{psi} \quad (26b)$$

$$J(270,60) = (0.294 + 0.0902) \times 10^{-6}$$
$$= 0.384 \times 10^{-6}/\text{psi} \quad (26c)$$

$$J(90,60) = (0.247 + 0.046) \times 10^{-6}$$
$$= 0.293 \times 10^{-6}/\text{psi} \quad (26d)$$

The corresponding creep coefficients $\varphi(t,t') = E(t')J(t,t') - 1$ are:

$$\varphi(18263,60) = 5.216 \times 10^6 \times 0.762 \times 10^{-6} - 1$$
$$= 2.975 \quad (27a)$$

$$\varphi(18083,60) = 5.216 \times 10^6 \times 0.763 \times 10^{-6} - 1$$
$$= 2.98 \quad (27b)$$

$$\varphi(270,60) = 5.216 \times 10^6 \times 0.384 \times 10^{-6} - 1$$
$$= 1.003 \quad (27c)$$

$$\varphi(90,60) = 5.216 \times 10^6 \times 0.293 \times 10^{-6} - 1$$
$$= 0.528 \quad (27d)$$

During the bridge's lifetime, its internal forces change substantially. Reference 38 shows how a theoretically exact solution of creep effects in a segmental box girder of arbitrarily non-uniform age and any construction procedure can be obtained by a step-by-step calculation. This method, however, is too tedious to execute without a computer.

Therefore, we will employ here the age-adjusted effective modulus method, which is simple and has been demonstrated to be quite accurate. Interested readers may consult References 9, 37, 38, and 39 for an explanation of the method.

The age-adjusted effective modulus E'' may be calculated with the aid of a table of the aging coefficient χ, which would have to be determined initially

for our creep function. We may, however, dispense with a table of χ and calculate E'' as:

$$E''(t,t') = \frac{E(t') - R(t,t')}{\varphi(t,t')} \tag{28}$$

where $R(t,t')$ is the relaxation function, for which recently a general and fairly accurate approximate formula has been established:[40]

$$R(t,t') = \frac{0.992}{J(t,t')} - \frac{0.115}{J(t,t-1)} \times \left(\frac{J(t'+\xi,t')}{J(t,t-\xi)} - 1 \right) \tag{29a}$$

where $\xi = (t-t')/2$ (29b)

To use Eq. (29) we need to know the following additional values, calculated similarly as before:

For $t = 18083, t' = 90$:

$$J_b(t'+\xi,t') = 0.409 \times 10^{-6}/\text{psi} \tag{30a}$$

where $\xi = 8996$ days, $J_b = E_o^{-1} + C_0 =$ part of J due to basic creep [Eq. (10)];

$$\bar{\varphi} = 11.12, S_d = 0.8055, \quad C_d = 0.243 \times 10^{-6}/\text{psi} \tag{30b}$$

$$J(t'+\xi,t') = (0.409 + 0.243) \times 10^{-6} = 0.652 \times 10^{-6}/\text{psi} \tag{30c}$$

$$J_b(t,t-\xi) = 0.2225 \times 10^{-6}/\text{psi} \tag{31a}$$

$$\bar{\varphi}_d = 9.5709, S_d = 0.80548, \quad C_d = 0.1028 \times 10^{-6}/\text{psi} \tag{31b}$$

$$J(t,t-\xi) = (0.2225 + 0.1028) \times 10^{-6} = 0.3253 \times 10^{-6}/\text{psi} \tag{31c}$$

For $t = 18263, t' = 270$:

$$J_b(t'+\xi,t') = 0.3395 \times 10^{-6}/\text{psi} \tag{32a}$$

$$\bar{\varphi}_d = 11.08, S_d = 0.8093, \quad C_d = 0.2054 \times 10^{-6}/\text{psi} \tag{32b}$$

$$J(t'+\xi,t') = (0.3395 + 0.2054) \times 10^{-6} = 0.5449 \times 10^{-6}/\text{psi} \tag{32c}$$

$$J_b(t,t-\xi) = 0.2221 \times 10^{-6}/\text{psi} \tag{33a}$$

$$\bar{\varphi}_d = 9.546, S_d = 0.8055, \quad C_d = 0.1022 \times 10^{-6}/\text{psi} \tag{33b}$$

$$J(t,t-\xi) = (0.2221 + 0.1022) \times 10^{-6} = 0.3243 \times 10^{-6}/\text{psi} \tag{33c}$$

For $t = 18,063, t' = 90$:

$$J_b(t,t') = 0.4432 \times 10^{-6}/\text{psi} \tag{34a}$$

$$\bar{\varphi}_d = 11.188, S_d = 0.8828, \quad C_d = 0.2662 \times 10^{-6}/\text{psi} \tag{34b}$$

$$J(t,t') = (0.3243 + 0.2662) \times 10^{-6} = 0.5905 \times 10^{-6}/\text{psi} \tag{34c}$$

For $t = 18263; t' = 270$:

$$J_b(t,t') = 0.3644 \times 10^{-6}/\text{psi} \tag{35a}$$

$$\bar{\varphi}_d = 11.08, S_d = 0.8828, \quad C_d = 0.2240 \times 10^{-6}/\text{psi} \tag{35b}$$

$$J(t,t') = (0.3644 + 0.2240) \times 10^{-6} = 0.5884 \times 10^{-6}/\text{psi} \tag{35c}$$

For $t = 18263, t' = t - 1$:

$$J_b(t,t') = 0.1369 \times 10^{-6}/\text{psi} \tag{36a}$$

$$\bar{\varphi}_d = 8.512, S_d = 0.04363, \quad C_d = 0.00445 \times 10^{-6}/\text{psi} \tag{36b}$$

$$J(t,t') = (0.1369 + 0.00445) \times 10^{-6} = 0.1414 \times 10^{-6}/\text{psi} \tag{36c}$$

For $t = 90, t' = t - 1$:

$$J_b(t,t') = 0.1841 \times 10^{-6}/\text{psi} \tag{37a}$$

$$\bar{\varphi}_d = 11.12, S_d = 0.04363, \quad C_d = 0.01318 \times 10^{-6}/\text{psi} \tag{37b}$$

$$J(t,t') = (0.1841 + 0.01318) \times 10^{-6} = 0.1973 \times 10^{-6}/\text{psi} \tag{37c}$$

For $t = 270, t' = t - 1$:

$$J_b(t,t') = 0.1672 \times 10^{-6}/\text{psi} \tag{38a}$$

$$\bar{\varphi}_d = 11.08, S_d = 0.04363, \quad C_d = 0.0111 \times 10^{-6}/\text{psi} \tag{38b}$$

$$J(t,t') = (0.1672 + 0.0111) \times 10^{-6} = 0.1783 \times 10^{-6}/\text{psi} \tag{38c}$$

Now, from Eq. (29):

$$R(18263,270) = (0.992/0.5884) - (0.115/0.1414) \times [(0.5449/0.3243) - 1] = 1.133 \times 10^6/\text{psi} \tag{39a}$$

$$R(18083,90) = \ldots = 0.5813 \times 10^6/\text{psi} \tag{39b}$$

$$E_a'' = E''(18263,270) = (5.982 - 1.133) \times 10^6/2.52 = 1.924 \times 10^6/\text{psi} \tag{39c}$$

$$E_b'' = E''(18083,90) = 1.704 \times 10^6/\text{psi} \tag{39d}$$

Note that the corresponding aging coefficients, which are used in References 9, 38, and 39 but are not needed here, are $(E - E'')/E''\,\phi$ or 0.849 and 0.770.

After joining the cantilevers at midspan, there are two statically indeterminate forces at midspan: shear force X_1 and bending moment X_2. Note that for a hinge connection, $X_2 = 0$; see Fig. 12. Using the principle of virtual work and evaluating the integrals by Simpson's rule, we obtain the following elastic flexibilities:

$$\delta_{11}^a = \delta_{11}^b = \int \frac{\overline{M}_1 \overline{M}_1}{EI}\,dx = \frac{\Delta x}{3E}\left(0 + 4\frac{12^2}{4.27} + 2\frac{24^2}{10.9} + 4\frac{36^2}{28.3} + \frac{48^2}{64.2}\right) = \frac{1839}{E}\left[\frac{1}{m}\right] \tag{40a}$$

$$-\delta_{12}^a = \delta_{12}^b = \int \frac{\overline{M}_1 \overline{M}_2}{EI}\,dx = \frac{\Delta x}{3E}\left(0 + 4\frac{12}{4.27} + 2\frac{24}{10.9} + 4\frac{36}{28.3} + \frac{48}{64.2}\right) = \frac{85.92}{E}\left[\frac{1}{m^2}\right] \tag{40b}$$

$$\delta_{22}^a = \delta_{22}^b = \frac{\Delta x}{3E}\left(0 + \frac{4}{4.27} + \frac{2}{10.9} + \frac{4}{28.3} + \frac{1}{64.2}\right) = \frac{5.109}{E}\left[\frac{1}{m^3}\right] \tag{40c}$$

$$\delta_1^q = -\delta_1^b = \int \frac{\bar{M}_1 M^L}{EI}\,dx = q\,\frac{\Delta x}{3E}\left(0 + 4\frac{12 \times 72}{4.27} + 2\frac{24 \times 288}{10.9} + 4\frac{36 \times 648}{28.3} + \frac{48 \times 1152}{64.2}\right) = 24950\frac{q}{E} \tag{40d}$$

$$\delta_2^q = \delta_2^b = -q\,\frac{\Delta x}{3E}\left(0 + 4\frac{72}{4.27} + 2\frac{288}{10.9} + 4\frac{648}{28.3} + \frac{1152}{64.2}\right) = 919.3\frac{q}{E}\left[\frac{1}{m}\right] \tag{40e}$$

In the above equations, the indices a, b refer to the left and right cantilevers; E = elastic modulus; $\overline{M}_1$, $\overline{M}_2$ = bending moments due to $X_1 = 1$ at $X_2 = 0$, and to $X_2 = 1$ at $X_1 = 0$; M_L = bending moments due to load q for $X_1 = X_2 = 0$; δ_1^q, δ_2^q = deflections due to load q in the direction of X_1 and X_2.

Note that here, similar to treating creep, we neglect the effect of reinforcement which is relatively small. To account for it one would have to calculate the transformed section properties for various moduli $E''(t,t')$ and $E(t')$ for concrete.

We must now write the conditions that the deformation increments in the direction of X_1 and X_2 from the time of joining to 50 years must be zero. According to the age-adjusted effective modulus method they read:[38]

$$(\delta_{11}^a E/E'' + \delta_{11}^b E/E'')X_1 + (\delta_{12}^a E/E_a'' + \delta_{12}^b E/E_b'')X_2 + (\delta_1^a \Delta\varphi_a + \delta_1^b \Delta\varphi_b)E/E(60) = 0 \tag{41a}$$

$$(\delta_{21}^a E/E_a'' + \delta_{21}^b E/E_b'')X_1 + (\delta_{22}^a E/E_a'' + \delta_{22}^b E/E_b'')X_2 + (\delta_2^a \Delta\varphi_a + \delta_2^b \Delta\varphi_b)E/E(60) = 0 \tag{41b}$$

Since $\Delta\varphi_a = \varphi(18263,60) - \varphi(270,60)$

$$= 2.975 - 1.003$$
$$= 1.972 \quad (42a)$$

$$\Delta\varphi_b = \varphi(18083,60) - \varphi(90,60)$$
$$= 2.98 - 0.528 = 2.452 \quad (42b)$$

We now have:

$$10^{-6}[(1.924^{-1} + 1.704^{-1})1839\,X_1/m + (-1.924^{-1} + 1.704^{-1})85.92\,X_2/m^2 + (1.972 - 2.452)24950\,q/5.216] = 0 \quad (43a)$$

$$10^{-6}[(-1.924^{-1} + 1.704^{-1})85.92\,X_1/m + (1.924^{-1} + 1.704^{-1})5.109\,X_2/m^2 - (1.972 + 2.452)919.3\,q/5.216] = 0 \quad (43b)$$

or

$$2035\,X_1 + 5.766\,X_2 = 2296[m^2]q \quad (44a)$$
$$5.766\,X_1 + 5.654\,X_2 = 780.0[m^2]q \quad (44b)$$

From the above, we can solve for the desired force and moment:

$$X_1 = 0.740q[m] = 103.6 \text{ kN} \quad (45a)$$
$$X_2 = 137.2q[m] = 19208 \text{ kNm} \quad (45b)$$

It is interesting to note that, relative to the end moment due to self weight for the case of no connection at midspan, the moment $\pm(48m)X_1$ due to X_1 represents ± 3.1 percent and X_2 represents 11.9 percent, causing the maximum change of the fixed-end moment to be 15.0 percent from joining to 50 years. A creep effect of this magnitude is certainly significant.

For an elastic structure upon which the load is applied after the final statical system (i.e., a system with a connection at midspan) is established, we would find $X_1 = 0$, $X_2 = 179.9q[m^2]$. We should note that the value of the midspan moment X_2 due to creep is 76 percent of this elastic value of X_2.

The deflection of the older cantilever at midspan at time of joining is:

$\Delta_1 = \delta_1^a\,\varphi(270,60)$ where δ_1^a is based on $E = E(60 \text{ days})$. Consequently:

$$\Delta_1 = (24950/5.216 \times 10^6 \text{ psi}) \times 1.003$$
$$= 0.0006957q[m^2/\text{kN}] = 0.0974 \text{ m} \quad (46)$$

The deflection from the instant of joining to 50 years may be calculated as:

$$\Delta_2 = (\delta_{11}^a X_1 + \delta_{12}^a X_2)E/E_a'' + \delta_1^a\,\Delta\varphi_a E/E(60)$$
$$= (1839 \times 0.740 - 85.92 \times 137.2q)/(1.924 \times 10^6) \text{ psi} + 24945q \times 1.972/(5.216 \times 10^6)$$
$$= 0.000582q/\text{kN} = 0.0814 \text{ m} \quad (47)$$

This value gives the total deflection due to self weight:

$$\Delta_1 + \Delta_2 = 0.0974 + 0.081 = 0.178 \text{ m}$$

Furthermore, one would have to calculate in a similar manner the values X_1, X_2 and deflections due to creep produced by the prestress. These tend to offset the above values and one may even obtain a design where they almost cancel each other. However, because of the statistical variability of each effect, it would be imprudent to rely in design on such "almost canceled values," as has often been done.

For comparison, if there were a hinge rather than a continuous connection at midspan, we would have:

$$X_2 = 0 \text{ and } 2035X_1 - 2296q[m^2] = 0$$

or

$$X_1 = 1.128q[m] = 158.0 \text{ kN}$$

The corresponding moment $(48m)X_1$ represents as much as 4.7 percent of the fixed-end moment for no connection at midspan, i.e., almost 1½-times as much as the 3.1 percent value found before, but about 3-times less than the total maximum change of 15.0 percent computed previously.

Also for comparison, if there were a hinge at midspan the deflection from joining to 50 years would be

$$\Delta_2 = \delta_{11}^a X_1 E/E_a'' + \Delta\varphi_a\delta_1^a E/E(60)$$
$$= (1839 \times 1.128)/1.924 \times 10^6 \text{ psi} + (24945 \times 1.972)/5.216 \times 10^6 \text{ psi}$$
$$= 0.00152q/\text{kN} = 0.21 \text{ m} \quad (48)$$

This deflection is 2.58-times larger than that for a continuous connection at midspan. The change of slope in the younger cantilever at the midspan hinge from the moment of joining to 50 years would be:

$$\theta_2 = \delta_{12}^b X_1 E/E_b'' + \Delta\varphi_b\delta_2^b E/E(60)$$
$$= (85.92 \times 1.128q)/1.704 \times 10^6 \text{ psi} + (919.3 \times 2.452)/5.216 \times 10^6 \text{ psi}$$
$$= 0.0099 \text{ radians} = 0.57 \text{ deg} \quad (49)$$

A somewhat smaller but opposite rotation occurs at the hinge in the older cantilever, causing relative rotation of more than 1 deg due to dead load. This rotation is reduced by creep caused by the prestress. Nevertheless, it is probable that a fast passage of a heavy truck at this change of slope may cause non-negligible vibrations. For this reason, and even more so because of the much larger deflections, it is imprudent to design the segmental bridge with hinges at midspan. Rather, one should always use continuous connections, even though one must then provide extra reinforcement or prestress to resist the positive midspan moment X_2. The reasons for avoiding the hinge become compelling if one considers the statistical variability of creep effects, currently ignored in codes and design practice; and we should now add some comments on this problem.

Although this is not done in practice, the designer should also calculate the 95 percent confidence limits on the foregoing creep effects. Based on the information supplied in this paper and Reference 4, this can be done for the overall statistical variability of concrete properties in the bridge.

To obtain these limits we consider all the preceding J-values to be 29 percent higher (see Table 1) and repeat all the calculations obtaining upper confidence limits on X_1, X_2, and deflections. Then we assume them to be 29 percent lower and repeat all calculations, obtaining the lower confidence limits. The effects of creep due to the prestressing forces (plus the effects of shrinkage) can be calculated in a similar manner, and their upper and lower confidence limits should be also established.

We must be aware, however, that we do not currently have a firm understanding on the statistical differences in creep between the upper and lower fibers of the cross section and between the left and right cantilevers. These statistical variations, which undoubtedly represent important causes of excessive deflections observed in concrete structures, are not mutually independent, and therefore the confidence limits for their differences must be less than those deduced on the basis of Table 1. Thus, one needs to obtain information on joint probability distributions within the cross section of the errors of creep in the upper and lower fibers of the section. Further research in this area is needed here.

Errors in the prediction of prestress loss are likewise very important. For example, we may have, as the mean prediction, a downward deflection of 20 cm due to self weight, and an upward deflection of 18 cm due to prestress, giving a net mean deflection of 2 cm. But if there is a 10 percent error in prestress, we have a downward deflection of $20 - 18(1 - 0.1) = 4$ cm. Hence, we see that a 10 percent error in prestress loss causes a 100 percent error in the net deflection. It is well known that a small difference of two large numbers is much more inaccurate than the numbers themselves, and the designer must be careful about this potential error.

Conclusions

1. Compared to the previous BP model,[4] the proposed model represents a simplified method for predicting creep characteristics which uses more limited material properties but fits test data less closely.

2. In terms of test data fits, the proposed model is the best one available for predicting the basic creep solely on the basis of concrete strength. This is useful when the designer has no idea of the concrete mix to be used.

3. Shrinkage cannot be satisfactorily predicted without using some composition parameters, and the designer must make at least a rough estimate of the composition to be used.

4. Because drying creep is always accompanied by shrinkage, it is better not to use a simpler (and a less accurate) formula for predicting it solely on the basis of strength.

5. If we measure one short-time shrinkage value (an average from several specimens), we can, however, generally predict shrinkage without using composition parameters, and with much better accuracy.

6. If we measure the value of the elastic modulus we can greatly improve the prediction of creep. The same is true if we measure one short-time creep value (average).

7. If we measure one short-time value of drying creep (average), we can generally predict drying creep without using composition parameters, and more accurately.

8. Explicit formulas for improved prediction based on two measured short-time values (average) are possible with the proposed model (including also the ACI model). However, models defined by graphs (e.g., the CEB-FIP method) are unsuitable for this purpose, and inconvenient for computer programs.

9. The proposed model compares distinctly better with test data than the ACI model as well as the new CEB-FIP Model Code (Table 1). It represents more of a compromise and never exhibits the very large deviations from some data as seen with the other two models. Moreover, the scope of the model is much broader. The improvement is greatest for long-time creep and higher ages at loading.

10. The earlier BP model, which fits the test data far better than the ACI model and the CEB-FIP model, is preferable to the present model when the composition of concrete is known.

11. The order of decreasing simplicity appears to be (a) Branson's (ACI 209) model;[2,3] (b) the proposed model, and the CEB-FIP Model Code,[1] and (c) earlier BP model.[4] Branson's (ACI 209) model, when suggested about a decade ago, represented the best possible model at that time, and it still remains nearly the best that can be done with the same degree of simplicity and under the constraint of using the same time shape for both basic and drying creep curves. Nevertheless, this simplicity is not worth the error in view of the great improvement achieved by the proposed model and especially the earlier BP model.

12. The CEB model fits shrinkage data less well than the ACI model but in fits of creep data it is somewhat better (Table 1), even though the current German Code DIN on which it is based is poorer. This was achieved by the adoption of a modification[36] in which a corrective initial term was determined by computer optimization.

13. The CEB-FIP and ACI models show much larger, and often unacceptable, errors, especially in cases of shrinkage, and the effects of humidity, size and curing period on shrinkage or creep. This is mainly because these phenomena are not modeled on the basis of diffusion theory but are derived empirically.

14. The general trend and shape of the creep and shrinkage curves in the proposed model, as well as the effect of loading age, are much more realistic than in the ACI or CEB-FIP models. This is important especially for extrapolations beyond the range of available test data.

15. The preceding point is corroborated by the fact that the error improvement for the proposed model, compared to the ACI and CEB models, is much more marked when test data for one particular concrete are fitted independently. The proposed model achieves much more improvement in the form of creep and shrinkage laws than it does in predicting material parameters from strength and composition of concrete. However, a possibility of further improvement in this area exists.

16. For experimental verification of a creep prediction model it is extremely important to avoid any subjective element in choosing the test data. By omitting four worst data sets among twelve, the coefficient of variation may drop to as low as one quarter.

17. The coefficients of variation and 95 percent confidence limits established here (Tables 1 and 2) enable the designer to determine the statistical parameters of the distribution of deflections, shrinkage stresses and strain redistributions in the structure due to creep, prestress losses, and other causes. The statistical variation of these effects is neglected in current practice but is actually much larger than the statistical variation of strength for which the current codes routinely account.

18. None of the creep prediction models proposed so far are too complicated for a creep-sensitive structure if one compares the analyst's time needed to calculate creep coefficients to that he routinely spends on structural analysis and considers the error originating from these two tasks.

19. The proposed model BP2 is advocated for consideration by code-preparing bodies as a basis for an improved practical prediction method to be used for creep-sensitive structures with normal concretes of strength 3000 to 6000 psi when a good estimate of concrete composition is not available. The earlier BP model[4] should be used, however, for all structures of high creep sensitivity, and generally whenever the concrete composition used is already known, because the gain in accuracy outweighs the increase in complexity. That model is also valid over a broader range of strengths and times.

Unit Equivalents

U.S. to metric (SI)

1 in. = 25.4 mm
1 ft = 0.3048 m
1 ft^2 = 0.0929 m^2
1 ft^3 = 0.02832 m^3
1 ft^4 = 0.00863 m^4
1 kip = 0.4448 kN
1 ksi = 1000 psi = 6.895 MN/m^2
= 6.895 MPa
1 psf = 4.788 N/m^2
= 4.788 Pa

Metric (SI) to U.S.

1 mm = 0.03937 in.
1 m = 3.281 ft
1 m^2 = 10.76 ft^2
1 m^3 = 35.31 ft^3
1 m^4 = 115.9 ft^4
1 kN = 2248 lb
= 2.248 kip
1 MN/m^2 = 1 MPa = 145 psi
= 0.145 ksi
1 N/m^2 = 1 Pa = 0.209 psf

REFERENCES

1. CEB-FIP Model Code for Concrete Structures, Commité Eurointernational du Béton—Fédération Internationale de la Précontrainte, CEB Bulletin No. 124/125-E, Paris 1978.
2. ACI Committee 209/II (chaired by D. E. Branson, "Prediction of Creep, Shrinkage and Temperature Effects in Concrete structures," ACI-SP27, *Designing for Effects of Creep, Shrinkage and Temperature,* American Concrete Institute, Detroit, 1971, pp. 51-93.
3. ACI Committee 209/II (chaired by D. Carreira), Revised Edition of Reference 2, 1978 (to be published).
4. Bažant, Z. P., and Panula, L., "Practical Prediction of Time-Dependent Deformations of Concrete," Materials and Structures, Parts I and II: V. 11, No. 65, 1978, pp. 307-328, Parts III and IV: V. 11, No. 66, 1978, pp. 415-434, Parts V and VI: V. 12, No. 69, 1979, pp. 169-183.
5. Bažant, Z. P., and Osman, E., "On the Choice of Creep Function for Standard Recommendations on Practical Analysis of Structures," *Cement and Concrete Research,* V. 5, 1975, pp. 129-138, 631-641; V. 6, pp. 149-153; V. 7, pp. 119-130; V. 8, pp. 129-130.
6. Bažant, Z. P., and Thonguthai, W., "Optimization Check of Certain Recent Practical Formulations for Concrete Creep," *Materials and Structures* (RILEM, Paris), V. 9, 1976, pp. 91-96.
7. Bažant, Z. P., and Kim, S. S., "Can the Creep Curves for Different Loading Ages Diverge?" *Cement and Concrete Research,* V. 8, September 1978, pp. 601-611.
8. Bažant, Z. P., and Panula, L., "A Note on Limitations of a Certain Creep Function Used in Practice," *Materials and Structures,* V. 12, No. 67, 1979, pp. 29-31.
9. Bažant, Z. P., "Theory of Creep and Shrinkage in Concrete Structures: A Précis of Recent Developments," *Mechanics Today,* Pergamon Press, V. 2, 1975, pp. 1-93.
10. Bažant, Z. P., and Osman, E., "Double Power Law for Basic Creep of Concrete," *Materials and Structures* (RILEM, Paris), V. 9, No. 49, 1976, pp. 3-11.
11. Bažant, Z. P., Osman, E., and Thonguthai, W., "Practical Formulation of Shrinkage and Creep of Concrete," *Materials and Structures* (RILEM, Paris), V. 9, No. 54, 1976, pp. 395-406.
12. Bažant, Z. P., and Najjar, L. J., "Non-Linear Water Diffusion in Non-saturated Concrete," *Materials and Structures* (RILEM, Paris), V. 5, 1972, pp. 3-20.
13. Hansen, T. C., and Mattock, A. H., "Influence of Size and Shape of Member on the Shrinkage and Creep of Concrete," *ACI Journal,* Proceedings V. 63,1966, pp. 267-290.
14. L'Hermite, R., and Mamillan, M., "Retrait et fluages des bétons," *Annales de l'Institut Technique du Bâtiment et des Travaux Publics (Supplément),* V. 21, No. 249, 1968, p. 1334; "Nouveaux résultats et récentes études sur le fluage du béton," *Materials and Structures,* V. 2, 1969, pp. 35-41; Mamillan, M., Bouineau, A., "Influence de la dimension des éprouvettes sur le retrait," *Annales Institut Technique du Bâtiment et des Travaux Publics (Supplément),* V. 23, No. 270, 1970, pp. 5-6.
15. Troxell, G. E., Raphael, J. M., and Davis, R. W., "Long-Time Creep and Shrinkage Tests of Plain and Reinforced Concrete," *Proceedings,* ASTM V. 58, 1958, pp. 1101-1120.
16. Keeton, J. R., "Study of Creep in Concrete," Technical Reports R333-I, R333-II, R333-III, 1965, U.S. Naval Civil Engineering Laboratory, Port Hueneme, California.
17. L'Hermite, R. G., Mamillan, M., and Lefèvre, C., "Nouveaux résultats de recherches sur la déformation et la rupture du béton," *Annales de l'Institut Technique du Bâtiment et des Travaux Publics,* V. 18, No. 207-208, 1965, pp. 323-360. See also International Conference on the Structure of Concrete, Cement and Concrete Association, London, 1968, pp. 423-433.
18. Hanson, J. A., "A Ten-Year Study of Creep Properties of Concrete," Concrete Laboratory Report No. SP-38, U.S. Department of the Interior, Bureau of Reclamation, Denver, Colorado, July 1953.
19. Harboe, E. M., *et al.,* "A Comparison of the Instantaneous and the Sustained Modulus of Elasticity of Concrete," Concrete Laboratory Report No. C-854, Division of Engineering Laboratories, U.S. Department of the Interior, Bureau of Reclamation, Denver, Colorado, March 1958.
20. Pirtz, D., "Creep Characteristics of Mass Concrete for Dworshak Dam," Report No. 65-2, Structural Engineering Laboratory, University of California, Berkeley, October 1968.
21. Browne, R. D., and Blundell, R., "The Influence of Loading Age and Temperature on the Long Term Creep Behaviour of Concrete in a Sealed, Moisture Stable State," *Materials and Structures* (RILEM, Paris), V. 2, 1969, pp. 133-143.
22. Browne, R. D., and Burrow, R. E. D., "Utilization of the Complex Multiphase Material Behavior in Engineering Design," In Structure, Solid Mechanics and Engineering Design, Civil Engineering Materials Conference held in Southampton, England, 1969, Edited by M. Te'eni, Wiley Interscience, 1971, pp. 1343-1378.
23. Browne, R. D., and Bamforth, P. P., "The Long Term Creep of the Wylfa P.V. Concrete for Loading Ages up to 12½ Years," 3rd International Conference on Structural Mechanics in Reactor Technology, Paper H 1/8, London, September 1975.
24. Rostasy, F. S., Teichen, K.-Th., and Engelke, H., "Beitrag zur Klärung des Zusammenhanges von Kriechen und Relaxation bei Normal-beton," Amtliche Forschungs-und Materialprüfungsanstalt für das Bauwesen. Otto-Graf-Institut, Universität Stuttgart, Strassenbau und Strassenverkehrstechnik, Heft 139, 1972.
25. McDonald, J. E., "Time-Dependent Deformation of Concrete Under Multiaxial Stress Conditions," Technical Report C-75-4, U.S. Army Engineer Waterways Experiment Station, Vicksburg, Mississippi, October 1975 to Oak Ridge National Laboratory, Oak Ridge, Tennessee 37830, Operated by Union Carbide Corporation for the U.S. Energy Research and Development Administration.
26. York, G. P., Kennedy, T. W., and Perry, E. S., "Experimental Investigation of Creep in Concrete Subjected to Multiaxial Compressive Stresses and Elevated Temperatures," Research Report 2864-2 to Oak Ridge National Laboratory operated by Union Carbide Corporation for U.S. Atomic Energy Commission, Department of Civil Engineering, the University of Texas at Austin, June 1970.
27. Lambotte, H., and Mommens, A., "L'Evolution du fluage du béton en fonction de sa composition, du taut et de l'age," Groupe de travail GT22, Centre National de Recherches Scientifiques et Techniques pour L'Industrie Cimentière, Bruxelles, July 1976.
28. Maity, K., and Meyers, B. L., "The Effect of Loading History on the Creep and Creep Recovery of Sealed and Unsealed Plain Concrete Specimens," Report No. 70-7 prepared under National Science Foundation Grant GK-3066, Department of Civil Engineering, University of Iowa, Iowa City, September 1970.
29. Hummel, A., Wesche, K., and Brand, W., "Der Einfluss der Zementart, des Wasser-Zement-Verhältnisses und des Belastungsalters auf das Kriechen von Beton," *Deutscher Ausschuss für Stahlbeton,* Heft 146, Berlin 1962. Vertrieb durch Verlag von Wilhelm Ernst und Sohn.
30. Branson, D. E., Meyers, B. L., and Kripanarayanan, K. M., "Time-Dependent Deformation on Non-composite and Composite Prestressed Concrete Structures," Highway Research Record No. 324, 1970, pp. 15-33.
31. Branson, D. E., and Christiason, M. L., "Time-Dependent Concrete Properties Related to Design Strength and Elastic Properties, Creep and Shrinkage," SP-27, *Designing for Creep, Shrinkage and Temperature,* American Concrete Institute, Detroit 1971, pp. 257-277.
32. Branson, D. E., *Deformations of Concrete Structures,* McGraw Hill, New York, 1977.
33. Rüsch, H., Jungwirth, D., and Hilsdorf, H., "Kritische Sichtung der Verfahren zur Berücksichtigung der Einflüsse von Kriechen," *Beton-und Stahlbetonbau* V. 68, 1973, pp. 49-60, 76-86, 152-158.
34. Rüsch, H., and Jungwirth, D., "Berücksichtigung der Einflüsse von Kriechen und Schwinden auf das Verhalten der Tragwerke," Werner-Verlag, Düsseldorf 1976.
35. CEB (Comité Européen du Béton), *3rd Draft of Model Code for Concrete Structures,* Bulletin d'Information No. 117-F, Paris, Dec. 1976.

36. Bažant, Z. P., Panula, L., "A Note on Amelioration of the Creep Function for Improved Dischinger Method," *Cement and Concrete Research*, V. 8, No. 3, 1978, pp. 381-386.
37. Bažant, Z. P., "Prediction of Concrete Creep Effects Using Age-Adjusted Effective Modulus Method," *ACI Journal*, V. 69, 1972, pp. 212-217.
38. Bažant, Z. P., and Najjar, L. J., "Comparison of Approximate Linear Methods for Concrete Creep," Journal of the Structural Division, Proc. ASCE, V. 99, No. ST9, September 1973, pp. 1851-1874.
39. Bažant, Z. P., Carreira, D. J., and Walser, A., "Creep and Shrinkage in Reactor Containment Shells," *Journal of the Structural Division*, Proceedings, ASCE, V. 101, No. ST10, October 1975, pp. 2118-2131.
40. Bažant, Z. P., and Kim, S. S, "Approximate Relaxation Function for Concrete," *Journal of the Structural Division*, Proceedings, ASCE, V. 105, 1979, pp. 2695-2705.
41. Bažant, Z. P., "Thermodynamics of Solidifying or Melting Viscoelastic Material," *Journal of the Engineering Mechanics Division*, Proceedings, ASCE, V. 105, 1979, pp. 933-952.
42. Bažant, Z. P., and Panula, L., "New Model for Practical Prediction of Creep and Shrinkage," A. Pauw Symposium on Designing for Creep and Shrinkage, held in Houston, November 1978, ACI Special Publication. (To be published by American Concrete Institute.)

* * *

Acknowledgment

Support by the U.S. National Science Foundation under Grant No. ENG77-06767 to Northwestern University is gratefully acknowledged.

The theoretical foundations underlying the proposed model were developed partly under a Guggenheim Fellowship awarded to the first author. The second author also received a fellowship of The Alumnae of Northwestern University.

* * *

APPENDIX A—CALCULATION OF CURVES FOR ACI AND CEB-FIP MODELS

ACI Model[2,3]

$$\epsilon_{sh}(\hat{t},t_0) = 0.00078\,\frac{\hat{t}}{55+\hat{t}}\,CF',\ CF' = c_1'c_2'c_3'c_4'c_5', \tag{50}$$

$$\text{for } h \leq 0.4: c_2' = 1;\ \text{for } h \geq 0.8: c_2' = 3 - 3h;\ \text{for } 0.4 < h < 0.8: c_2' = 1.4 - h \tag{51}$$

$$c_3' = 1.2\,e^{-0.0473\,v/s},\ c_4' = 0.75 + 0.00061\,c \tag{52}$$

$$c_5' = 0.3 - 1.4\,\frac{s}{a}\ \text{ for }\ \frac{s}{a} \leq 0.5,\ \text{else } c_5' = 0.9 - 0.2\,\frac{s}{a} \tag{53}$$

$$J(t,t') = \frac{1+C_t}{E(t')},\ E(t') = 33\sqrt{\rho^3 f_c'(t')},\ f_c'(t') = f_{c28}'\,\frac{t'}{4+0.85t'},\ t' \geq 7\ \text{days} \tag{54}$$

$$C_t = \frac{(t-t')^{0.6}}{10+(t-t')^{0.6}}\,C_u,\ C_u = 2.35\,CF,\ CF = c_1c_2c_3c_4 \tag{55}$$

$$c_1 = 1.25\,t'^{-0.118};\ c_2 = 1.27 - 0.67\,h \text{ for } h > 0.4,\ \text{else } c_2 = 1.00; \tag{56}$$

$$c_3 = \frac{2}{3}\,(1 + 1.13\,e^{-0.212\,v/s}),\ c_4 = 0.88 + 0.0024\,\frac{s}{a} \tag{57}$$

Note that c_1' is a function of initial moist curing defined by Table 2.8 in Reference 3. Here ρ = unit mass of concrete in lb/ft³; CF, CF' = correction factors, c = cement content in kg/m³, v/s = volume to surface ratio in cm, s/a = ratio of the fine aggregate (sand) content to the total aggregate content (by weight). The slump and air content influences[3] were not considered for the data in the figures because their values were not reported for most data considered.

CEB-FIP Model Code[1]

$$\epsilon_{sh} = \epsilon_{s_0}[\beta_s(t) - \beta_s(t_0)],\ \epsilon_{s_0} = \epsilon_{s_1}\epsilon_{s_2},\ H_0 = \lambda\,\frac{2A_c}{U} \tag{58}$$

The strain ϵ_{s_1} is defined by Table 0.1, Column 4 in Reference 1 as a function of humidity h; ϵ_{s_2} is defined by a graph in Fig. e.4 as a function of H_0; A_c/U = ratio of cross-sectional area to exposed surface; λ is a function of h defined by Table e.1; $\beta_s(t)$ = function of age t defined by six graphs in Fig. e.6 for various values of effective thickness H_0. Age t was not corrected for temperature (Section e.5 of Reference 1) because the test temperatures did not differ appreciably from 20C.

$$J(t,t') = \frac{1}{E_c(t')} + \frac{\beta_a(t')}{E_{c_{28}}} + \frac{\varphi_d\beta_d(t,t')}{E_{c_{28}}} + \frac{\varphi_f[\beta_f(t) - \beta_f(t')]}{E_{c_{28}}} \tag{59}$$

$$\beta_a(t') = 0.8\left(1 - \frac{f_c'(t')}{f_{c_\infty}'}\right),\ \varphi_d = 0.4,\ \varphi_f = \varphi_{f_1}\varphi_{f_2} \tag{60}$$

$$E_c(t') = 1.25\,E_{c_m}(t'),\ E_{c_m}(t') = 9500\sqrt[3]{f_{c_m}'(t')},\ E_{c_{28}} = 9500\sqrt[3]{f_c'} \tag{61}$$

where f_{c_m}', E_{c_m} and E are in N/mm². The strength f_c' is given by a graph in Fig. e.1 of Reference 1 as a function of t'; φ_{f_1} is given in Table e.1 of Reference 1 as a function of humidity h; φ_{f_2} is given by a graph in Fig. e.2 of Reference 1 as a function of effective thickness H_0; β_d is defined by a graph in Fig. e.3 of Reference 1 as a function of load duration $t - t'$, β_f is given by six graphs in Fig. e.4 for various effective thicknesses H_0 (Table 2.3 of Reference 1) as a function of age t, which does not have to be here corrected for temperature as already noted.

Compared to German Code DIN[33,34] and the preliminary version from Reference 35, the modification proposed in Reference 36 and embodied in the above equations consists of replacing the actual elastic deformation $1/E_c(t')$ with the term $1/E_{ic}(t') = 0.46(1 + 3.22\,t'^{-0.4})/E_{c_{28}}$ where $E_{ic}(t')$ was called "initial creep modulus."[29] In the Model Code the proposed change from $1/E_c(t')$ to $1/E_{ic}(t')$ is hidden within the term $\beta_a(t')/E_{c_{28}}$ which is called "irreversible initial deformation" and is given as $0.8[1 - f_c'(t')/f_{c_\infty}']$ where $f_c'(t')$ is given by a graph such that this term is equivalent to the originally proposed[36] function $1/E_{ic}(t')$ minus $1/E_c(t')$, i.e., $f_c'(t')/f_{c_\infty}' \approx 1 - [1/E_{ic}(t') - 1/E_{ic_{28}}]/0.8$.

APPENDIX B—NOTATION

a/c = aggregate-cement ratio (by weight)
$C_0(t,t')$ = unit basic creep strain (in excess of $1/E_0$, not $1/E$)
$C_1(t_0)$ = drying diffusivity of nearly saturated concrete at reference temperature T_o at age t
$C_d(t,t',t_0)$ = increase of creep during drying
D = effective cross-section thickness
E = Young's modulus of concrete
$E_{28} = E$ at $t' = 28$ days
E_o = asymptotic modulus of concrete
f'_c = 28-day cylinder strength of concrete
g/s = gravel-sand ratio (by weight)
h = relative humidity of the environment $(0 \leq h \leq 1)$
$J(t,t')$ = strain at time t caused by a unit sustained uniaxial stress acting since time t'
k_h = humidity coefficient
k'_h = humidity coefficient
k_S = shape factor
m = material parameter
n = material parameter
r = parameter
RH = relative humidity (in percent)
s/a = sand-aggregate ratio (by weight)
s/c = sand-cement ratio (by weight)
$S(\hat{t})$ = function giving shape of shrinkage curve
$S_d(t,t')$ = shrinkage-like time shape function for increase of creep due to drying
t = time in days representing the age of concrete
t' = age of concrete at loading in days
t_0 = age of concrete when drying begins
t = duration of drying
v/s = volume-to-surface ratio
w/c = water-cement ratio
y = parameter
z = parameter
α = material parameter
$\epsilon_{sh}(\hat{t},t_o)$ = shrinkage strain
ϵ_{sh_∞} = ultimate shrinkage (at zero humidity)
τ_{sh} = shrinkage square half time
φ_1 = material parameter
φ_d = material parameter
$\bar{\varphi}$ = coefficient characterizing the increase due to drying

* * *

Discussion of this paper is invited.
Please submit your comments to
PCI Headquarters by January 1, 1981.